

# Dynamics and stability of spike-type solutions to a one dimensional Gierer-Meinhardt model with sub-diffusion

Yana Nec\* and Michael J. Ward

Department of Mathematics, University of British Columbia  
1984 Mathematics Road, Vancouver, V6T1Z2, BC, Canada

\* *email: oulanka@math.ubc.ca*

## Abstract

The dynamics and stability of spike-type patterns to a sub-diffusive Gierer-Meinhardt reaction – diffusion system is studied in a one dimensional spatial domain. A differential algebraic system (DAE) is derived to characterise the dynamics of an  $n$ -spike quasi-equilibrium pattern in the presence of sub-diffusion. With sub-diffusive effects it is shown that quasi-equilibrium spike patterns exist for diffusivity ratios asymptotically smaller than for the case of regular diffusion, and that the spikes approach their equilibrium locations at an algebraic, rather than exponential, rate in time.

A new non-local eigenvalue problem (NLEP) is derived to examine the stability of an  $n$ -spike pattern. For a two-spike pattern sub-diffusion has little effect on the competition instability threshold, whereas the threshold associated with an oscillatory instability of the spike profile increases significantly. Furthermore, for a multi-spike pattern it is shown that an asynchronous oscillatory instability of the spike profile, rather than a synchronous oscillatory instability characteristic of the case of regular diffusion, is the dominant instability when the anomaly index  $\gamma$  is below a certain threshold. Detailed numerical results are presented for the two-spike case.

*Keywords:* sub-diffusion, fractional derivative, spike solution, non-local eigenvalue problem, anomaly exponent.

## 1 Introduction

Sub-diffusion is a diffusion anomaly, whereby the mean square displacement of the diffusing particle evolves according to  $\langle r^2(t) \rangle \sim t^\gamma$ , with  $0 \leq \gamma < 1$  being the anomaly index. Adopting the concept of a continuous time random walk for the description of diffusion, the probability to make a step of length  $r$  after time  $t$  is given by

$$\psi(r, t) = w(t) m(r),$$

where  $w(t)$  and  $m(r)$  are the waiting time and step length probability density functions, respectively. Regular diffusion, associated with  $\langle r^2(t) \rangle \sim t$ , ensues when  $w(t) = \frac{1}{\tau_*} e^{-t/\tau_*}$ , where  $0 < \tau_* \sim \mathcal{O}(1)$  is a characteristic time scale, and  $m(r)$  is Gaussian. The sub-diffusive behaviour arises when the exponential waiting time probability function is replaced by an algebraic function

$$w(t) = \frac{\gamma \tau_*^\gamma}{(t + \tau_*)^{\gamma+1}}, \quad 0 < \tau_* \sim \mathcal{O}(1).$$

Since  $\tau_*$  does not affect the asymptotics of the mean square displacement, it is often set to  $\tau_* = 1$ .

Sub-diffusion has been observed in nature and in particular in biological systems, where the diffusion is often hindered due to the complex structure of either the particle or the medium (cf. [1, 2, 3]). Owing to advances in techniques used in scientific measurement, the exponent  $\gamma$  has been accurately estimated in an ever increasing number of experimental situations. These experimental results have confirmed that the regular Fickian-type diffusion is only a special limit of a whole family of processes. The continuum limit operator  $\partial_t - \nabla^2$  in the diffusion equation is then replaced by a fractional operator  $\partial_t^\gamma - \nabla^2$  (cf. [4]).

The fractional derivative is a generalisation of the usual integer derivative to an arbitrary order, and is usually defined as (cf. [5])

**Definition 1.1**

$$\frac{d^\gamma}{dt^\gamma} f(t) = \frac{d^n}{dt^n} \frac{d^{\gamma-n}}{dt^{\gamma-n}} f(t) = \frac{1}{\Gamma(n-\gamma)} \frac{d^n}{dt^n} \int_a^t \frac{f(\zeta) d\zeta}{(t-\zeta)^{\gamma-n+1}}, \quad n-1 \leq \gamma < n, \quad n \in \mathbb{N}, \quad a \in \mathbb{R}.$$

In the context of a temporal derivative, the lower bound of the integral is usually set to  $a = 0$ . The operator order relevant to sub-diffusion is  $0 \leq \gamma < 1$ . A similar definition to be used in this paper is

**Definition 1.2**

$$\frac{d^\gamma}{dt^\gamma} f(t) = -\frac{1}{\Gamma(-\gamma)} \int_0^t \frac{f(t) - f(t-\zeta)}{\zeta^{\gamma+1}} d\zeta, \quad 0 \leq \gamma < 1.$$

The upper limit in the integral is sometimes taken to be infinite, in which case it is implied that  $f(t) = 0$  for  $t < 0$ . The limit  $\gamma \rightarrow 0^+$  corresponds to a stagnant medium. The limit  $\gamma \rightarrow 1^-$  corresponds to regular diffusion. Both limits are improper in the sense that the first derivative cannot be obtained directly from Definition 1.2. It is possible to show the equivalence of  $\frac{d^\gamma}{dt^\gamma}$  in the limit  $\gamma \rightarrow 1^-$  and  $\frac{d}{dt}$  by using an alternative definition of the fractional operator that employs the Riemann sum, which is known as the Grünwald-Letnikov formulation (see [5]).

An operator of the type given by Definition 1.2 is referred to as a memory operator, since it takes into account the entire evolution history of the function  $f$ , as opposed to the case of the usual integer derivative. The immediate physical consequence is that there is an infinite first moment of the residence time in the random walk corresponding to the diffusion process (cf. [4]). The mean square displacement is then given by  $\langle r^2(t) \rangle \sim t^\gamma$ .

Fractional diffusion equations have been used to model anomalously slow or fast scattering of particles in a variety of natural applications (cf. [4]). The methods of solution of such equations often use integral transforms and special functions for the representation of fundamental solutions (cf. [6, 7]). Inclusion of a reaction term presents more challenges due to the inapplicability of many basic analytical tools and notions (e.g. chain rule, residue theorem, spectrum, Sturm-Liouville theory) in the context of fractional derivatives (cf. [8, 9]). In past studies, non-linear equations have been solved either numerically or asymptotically, except for the case where the qualitative form of the non-linearity was approximated by piecewise linear kinetics (cf. [9]). To the authors' knowledge, there have been no analytical studies of the stability of any spatially inhomogeneous solutions of such models. In the case of spatially uniform equilibria the use of dynamical systems methods for the analysis of problems with anomalous diffusion have reported intricate and somewhat counter-intuitive stability characteristics (cf. [10, 11, 12]).

The main goal of this paper is to characterise analytically the dynamics and stability of a spatially localised pattern of spike-type solutions for an activator – inhibitor system subject to sub-diffusion. Spike patterns for a singularly perturbed reaction – diffusion system in one spatial dimension are characterised by the concentration of one or more of the solution components near a discrete set of spatial locations in the domain. For quasi-equilibrium patterns these concentration points will evolve slowly in time. For the case of regular diffusion the dynamics and stability of such 1-D patterns have been extensively studied over the past decade for various models including the Gray-Scott and Gierer-Meinhardt models (cf. [13]–[26]).

A well known reaction – diffusion system for the generation of spike-type solutions is the activator-inhibitor system with Gierer-Meinhardt kinetics, given in a dimensionless form by

$$\partial_t a = \epsilon^2 a_{xx} - a + \frac{a^p}{h^q}, \quad \tau \partial_t h = D h_{xx} - h + \epsilon^{-1} \frac{a^m}{h^s}, \quad (1)$$

where  $a(x, t)$  and  $h(x, t)$  are the activator and inhibitor concentrations, respectively. Here  $\epsilon^2$  and  $D$  denote the constant diffusivities,  $\tau > 0$  is the reaction time constant, and the exponents  $(p, q, m, s)$  satisfy

$$p > 1, \quad q > 0, \quad m > 0, \quad s \geq 0, \quad 0 < \frac{p-1}{q} < \frac{m}{s+1}.$$

The stability properties of equilibrium spike patterns for (1) were studied in [14], [17], [20], and [21]. An analysis of slow dynamics of quasi-equilibrium spike patterns for (1) was given in [18], [24], and [25].

In this paper a modification of (1), incorporating sub-diffusion, is studied. The modified system on a one dimensional interval with Neumann boundary conditions has the form

$$\partial_t^\gamma a = \epsilon^{2\gamma} a_{xx} - a + \frac{a^p}{h^q}, \quad -1 < x < 1, \quad t > 0, \quad (2a)$$

$$\tau \partial_t^\gamma h = D h_{xx} - h + \epsilon^{-\gamma} \frac{a^m}{h^s}, \quad -1 < x < 1, \quad t > 0, \quad (2b)$$

$$a_x(\pm 1, t) = h_x(\pm 1, t) = 0, \quad a(x, 0) = a_0(x), \quad h(x, 0) = h_0(x), \quad (2c)$$

where the anomaly exponent  $\gamma$  is on the range  $0 < \gamma < 1$ .

The  $\gamma$ -dependent powers of  $\epsilon$  in the activator diffusivity and inhibitor non-linearity in (2) are essential for the existence of a quasi-equilibrium spike pattern. Upon substituting  $\gamma = 1$  the usual GM model (1) is recovered. The limit  $\gamma \rightarrow 0^+$  is improper since the function  $\epsilon^\gamma$  is arbitrarily small for  $\epsilon \rightarrow 0$  if  $0 < \gamma < 1$ , whereas  $\epsilon^\gamma = 1$  for arbitrarily small  $\epsilon$  when  $\gamma = 0$ .

In §2 a quasi-equilibrium spike solution to (2) is constructed, and a differential algebraic (DAE) system for the dynamics of spikes under the effect of sub-diffusion is derived. In §3 a non-local eigenvalue problem (NLEP) characterising the stability of an equilibrium spike pattern is derived. Studying this NLEP for a one-spike solution, it is shown that the effect of sub-diffusion is to increase the critical value of  $\tau$  for the onset of a Hopf bifurcation. Therefore, the effect of sub-diffusion is to broaden the parameter range where a stable equilibrium spike pattern can occur. Furthermore, for a multi-spike equilibrium solution, it is shown that an asynchronous oscillatory instability of the spike profile, rather than a synchronous oscillatory instability characteristic of the case of regular diffusion, is the dominant instability when the anomaly index  $\gamma$  is below a certain threshold. Detailed numerical results are presented for the two-spike case.

## 2 Dynamics of quasi-equilibrium patterns

In the limit  $\epsilon \rightarrow 0$  a solution to (2) is constructed, for which the activator concentrates at a finite set of locations  $x_i$  for  $i = 1, \dots, n$ , where  $x_i$  is the centre of the  $i$ -th spike. The background solution for (2a) in between each of the spikes is the trivial state  $a(x, t) \equiv 0$ . In the inner region near each  $x_i$  an inner coordinate  $y_i$  is defined by

$$y_i(t) \equiv \epsilon^{-\gamma} (x - x_i(\sigma)), \quad i = 1, \dots, n, \quad (3)$$

where  $\sigma = \epsilon^\alpha t$ , with  $\alpha > 0$  being a slow time scale to be determined. In order to derive a DAE system for the spike layer locations  $x_i(\sigma)$ , the following auxiliary result is needed.

**Lemma 2.1** Let  $A(y_i(\sigma)) \in C^\infty$  with  $y_i$  as in (3),  $x_i \in C^\infty$  and  $0 < \gamma < 1$ . Then in the limit  $\epsilon \rightarrow 0$  the chain differentiation rule is given by

$$\partial_\sigma^\gamma A(y_i(\sigma)) \sim -\epsilon^{-\gamma^2} \operatorname{sgn}\left(\frac{dx_i}{d\sigma}\right) \left|\frac{dx_i}{d\sigma}\right|^\gamma \mathfrak{D}_{y_i}^\gamma A(y_i),$$

where  $\mathfrak{D}_{y_i}^\gamma A(y_i)$  is defined by

$$\mathfrak{D}_{y_i}^\gamma A(y_i) \equiv \operatorname{sgn}\left(\frac{dx_i}{d\sigma}\right) \frac{1}{\Gamma(-\gamma)} \int_0^\infty \left\{ A(y_i) - A\left(y_i + \operatorname{sgn}\left(\frac{dx_i}{d\sigma}\right) \xi\right) \right\} \frac{d\xi}{\xi^{\gamma+1}},$$

and  $\Gamma(z)$  is the Gamma function.

PROOF : By Definition 1.2 one has

$$\partial_\sigma^\gamma A(y_i(\sigma)) = -\frac{1}{\Gamma(-\gamma)} \int_0^\sigma \left\{ A\left(\frac{x - x_i(\sigma)}{\epsilon^\gamma}\right) - A\left(\frac{x - x_i(\sigma - \zeta)}{\epsilon^\gamma}\right) \right\} \frac{d\zeta}{\zeta^{\gamma+1}}. \quad (4)$$

A new variable  $\xi$  in terms of  $\zeta$  is then defined by

$$\xi \equiv \epsilon^{-\gamma} (x_i(\sigma - \zeta) - x_i(\sigma)). \quad (5)$$

To solve for  $\zeta$  in terms of  $\xi$  when  $\epsilon \ll 1$ ,  $x_i$  is expanded ( $x_i \in C^\infty$ ) as

$$x_i(\sigma - \zeta) = x_i(\sigma) - \frac{dx_i}{d\sigma} \zeta + \frac{1}{2} \frac{d^2 x_i}{d\sigma^2} \zeta^2 - \dots,$$

so that (5) becomes

$$\xi = \epsilon^{-\gamma} \left( -\frac{dx_i}{d\sigma} \zeta + \frac{1}{2} \frac{d^2 x_i}{d\sigma^2} \zeta^2 - \dots \right).$$

Away from the fixed points, the series is reverted to leading order to get

$$\zeta = -\left(\frac{dx_i}{d\sigma}\right)^{-1} \left( \epsilon^\gamma \xi - \frac{1}{2} \frac{d^2 x_i}{d\sigma^2} \zeta^2 + \dots \right), \quad \frac{dx_i}{d\sigma} \neq 0,$$

and, thus, by a recursive substitution into higher powers of  $\zeta$  one derives that

$$\zeta \sim \epsilon^\gamma \left( -\frac{dx_i}{d\sigma} \right)^{-1} \xi + \mathcal{O}(\epsilon^{2\gamma}).$$

Therefore, for  $\epsilon \ll 1$  (4) becomes

$$\partial_\sigma^\gamma A(y_i(\sigma)) \sim -\frac{\epsilon^{-\gamma^2}}{\Gamma(-\gamma)} \left( -\frac{dx_i}{d\sigma} \right)^{-1} \int_0^{-\infty \cdot \operatorname{sgn}\left(\frac{dx_i}{d\sigma}\right)} \left( A(y_i) - A(y_i - \xi) \right) \left( -\frac{dx_i}{d\sigma} \frac{1}{\xi} \right)^{\gamma+1} d\xi.$$

Finally, upon splitting this result into the two cases  $\frac{dx_i}{d\sigma} \leq 0$  and changing variables to have the upper integration bound positive, the desired result is obtained.  $\blacksquare$

**Remark 2.1** The operator  $\mathfrak{D}_{y_i}^\gamma$  can be regarded as the left and right propagating fractional derivative according to whether  $\frac{dx_i}{d\sigma} \leq 0$ , and it satisfies  $\lim_{\gamma \rightarrow 1^-} \mathfrak{D}_{y_i}^\gamma = \frac{d}{dy_i}$ . The infinite integration bound appeared when the limit  $\epsilon \rightarrow 0$  was taken. Therefore, in the case of the left propagating fractional derivative the argument of  $A(y_i - \xi)$  becomes negative for fixed  $y_i$  and sufficiently large  $\xi$ , whence  $A$  should be regarded as vanishing.

**Lemma 2.2** For  $p > 1$ , the homoclinic solution  $u$ , given by

$$u(y) = \left\{ \left( \frac{p+1}{2} \right) \operatorname{sech}^2 \left( \frac{(p-1)}{2} y \right) \right\}^{\frac{1}{p-1}},$$

is the unique solution to the boundary value problem

$$u'' - u + u^p = 0, \quad -\infty < y < \infty, \quad u'(0) = 0, \quad u(0) > 0, \quad \lim_{|y| \rightarrow \infty} u = 0.$$

The corresponding linearised operator  $\mathcal{L}_0 \equiv \frac{d^2}{dy^2} - 1 + pu^{p-1}$ , subject to the same asymptotic boundary conditions, has a unique positive eigenvalue and a one dimensional nullspace with  $\operatorname{Ker} \mathcal{L}_0 = \operatorname{span}\{u'\}$ .

PROOF : Suppose  $u' \in \operatorname{Ker} \mathcal{L}_0$ . By a direct computation  $\mathcal{L}_0 u' = 0$ . Next, suppose that  $\mathcal{L}_0 \tilde{u} = 0$ . By the ODE existence and uniqueness theorem there are two independent solutions. One is  $\tilde{u}_1 = u'$ , satisfying  $\lim_{|y| \rightarrow \infty} \tilde{u}_1 = 0$  and  $\lim_{|y| \rightarrow \infty} \tilde{u}'_1 = 0$ . The other solution must satisfy  $\lim_{|y| \rightarrow \infty} |u| > 0$ , and in fact must blow up exponentially at infinity, since the Wronskian of these two independent solutions is non-zero in the limit  $|y| \rightarrow \infty$ . Since  $u > 0$  and is an even function, the derivative  $u'(y)$  has a unique zero at  $y = 0$ . Then, by Sturm-Liouville theory, there exists exactly one eigenpair of  $\mathcal{L}_0 \phi = \nu \phi$  with  $\nu = \nu_{\text{loc}} > 0$ , which has a corresponding eigenfunction of one sign. ■

The formal result below characterises the slow dynamics of a quasi-equilibrium  $n$  spike solution to (2).

**Principal result 2.1** Let  $x_i(\sigma) \in C^\infty$  be the location of the centre of the  $i$ -th spike, evolving on the slow time scale  $\sigma = \epsilon^\alpha t$  with  $\alpha = \gamma + 1$ . Suppose that  $\tau \sim o(\epsilon^{-(\gamma+1)\gamma})$ . Then in each inner region the quasi-equilibrium solution for (2) is given asymptotically for  $\epsilon \rightarrow 0$  by

$$A(y_i, \sigma) = a(x_i + \epsilon^\gamma y_i, \epsilon^{-\alpha} \sigma) = A_i^{(0)} + \epsilon^\gamma A_i^{(1)} + \dots \quad (6a)$$

$$H(y_i, \sigma) = h(x_i + \epsilon^\gamma y_i, \epsilon^{-\alpha} \sigma) = \bar{H}_i(\sigma) + \epsilon^\gamma H_i^{(1)} + \dots, \quad (6b)$$

where  $\bar{H}_i = \bar{H}_i(\sigma)$  and  $x_i(\sigma)$  satisfy the differential-algebraic (DAE) system

$$\bar{H}_i(\sigma) = b_m \sum_{j=1}^n \bar{H}_j^{\beta m - s} G(x_i; x_j), \quad b_m \equiv \int_{-\infty}^{\infty} u^m dy,$$

$$\operatorname{sgn} \left( \frac{dx_i}{d\sigma} \right) \left| \frac{dx_i}{d\sigma} \right|^\gamma = -\frac{qb_m}{(p+1)\bar{H}_i} \left\{ \bar{H}_i^{\beta m - s} \langle G_x \rangle_i + \sum_{\substack{j=1 \\ j \neq i}}^n \bar{H}_j^{\beta m - s} G_x(x_i; x_j) \right\} f(p; \gamma), \quad (7a)$$

where  $\langle G_x \rangle_i \equiv \frac{1}{2} (G_x(x_i^-; x_i) + G_x(x_i^+; x_i))$ . Here  $G(x; x_i)$  is the Green's function satisfying

$$DG_{xx} - G = -\delta(x - x_i), \quad -1 < x < 1; \quad G_x(\pm 1; x_i) = 0, \quad (7b)$$

while the anomaly dependent factor  $f(p; \gamma)$  is defined by

$$f(p; \gamma) \equiv \left( \int_{-\infty}^{\infty} u^{p+1} dy_i \right) / \left( \int_{-\infty}^{\infty} u'(y_i) \mathfrak{D}_{y_i}^\gamma u dy_i \right). \quad (7c)$$

The derivative  $\mathfrak{D}_{y_i}^\gamma$  is defined as in Lemma 2.1.

To derive this result first note that Definition 1.2 with  $f(t) \equiv F(\epsilon^\alpha t) = F(\sigma)$  implies that the fractional derivative satisfies  $\partial_t^\gamma f(t) = \epsilon^{\gamma\alpha} \partial_\sigma F(\sigma)$ . Thus, substituting (6) into (2) gives the leading order problem on as

$$\left(\frac{\partial^2}{\partial y_i^2} - 1\right) A_i^{(0)} + \frac{A_i^{(0)p}}{\bar{H}_i^q} = 0, \quad \frac{\partial^2}{\partial y_i^2} \bar{H}_i = 0, \quad -\infty < y_i < \infty. \quad (8)$$

This system has no dependence on  $\gamma$ , and as for the case of regular diffusion, the linear growth in  $y_i$  at infinity for  $\bar{H}_i$  must be eliminated in order to match to the outer solution. Thus,  $\bar{H}_i$  is independent of  $y_i$ , and

$$\bar{H}_i = \bar{H}_i(\sigma) > 0, \quad A_i^{(0)} = \bar{H}_i^\beta(\sigma) u(y_i), \quad \beta \equiv \frac{q}{p-1}, \quad (9)$$

where the homoclinic solution  $u$  is as in Lemma 2.2.

The error in this leading order approximation is of order  $\mathcal{O}(\epsilon^\gamma)$ . At the next order, the problem for  $A_i^{(1)}$  must involve the motion of the spike centre  $x_i$ . Normally the latter is obtained by the differentiation of  $A_i^{(0)}(y_i(\sigma), \sigma)$  with respect to the first argument together with an application of the chain rule involving  $\frac{dx_i}{d\sigma}$ . The derivative with respect to the second argument is of order of magnitude smaller. This procedure cannot be performed when the derivative is fractional. Applying Lemma 2.1 and using (9), the time scale is chosen as  $\alpha = \gamma + 1$  to obtain that the correction equations are

$$\bar{H}_i^{-\beta} \mathcal{L}_0 A_i^{(1)} = \frac{q}{\bar{H}_i} u^p H_i^{(1)} - \text{sgn} \left( \frac{dx_i}{d\sigma} \right) \left| \frac{dx_i}{d\sigma} \right|^\gamma \mathfrak{D}_{y_i}^\gamma u, \quad (10a)$$

$$D \frac{\partial^2}{\partial y_i^2} H_i^{(1)} = -\bar{H}_i^{\beta m - s} u^m. \quad (10b)$$

The time derivative term  $\tau \partial_t^\gamma \bar{H}_i$  in (2b) was neglected to obtain the problem for  $H_i^{(1)}$ . This is consistent when  $\tau \partial_t^\gamma \bar{H}_i \sim o(\epsilon^{-\gamma})$ . Since  $\partial_t^\gamma \bar{H}_i = \epsilon^{\alpha\gamma} \partial_\sigma^\gamma \bar{H}_i$  and  $\alpha = \gamma + 1$ , this condition holds when  $\tau$  satisfies  $\tau \sim o(\epsilon^{-\gamma(2+\gamma)})$ .

Upon using Lemma 2.2, together with the Fredholm alternative, and noting that  $\mathcal{L}_0$  is self-adjoint, the solvability condition is obtained

$$\int_{-\infty}^{\infty} \frac{du}{dy_i} \left\{ \frac{q}{\bar{H}_i} u^p H_i^{(1)} - \text{sgn} \frac{dx_i}{d\sigma} \left| \frac{dx_i}{d\sigma} \right|^\gamma \mathfrak{D}_{y_i}^\gamma u \right\} dy_i = 0. \quad (11)$$

The first term in (11) is integrated by parts twice and simplified by using the exponential decay of  $u$  at infinity, together with the facts that  $u$  and  $\partial_{y_i}^2 H_i^{(1)}$  are even functions. Then, the solvability condition becomes

$$\frac{q}{2(p+1)\bar{H}_i} \int_{-\infty}^{\infty} u^{p+1} dy_i \left( \lim_{y_i \rightarrow \infty} \frac{dH_i^{(1)}}{dy_i} + \lim_{y_i \rightarrow -\infty} \frac{dH_i^{(1)}}{dy_i} \right) = - \left| \frac{dx_i}{d\sigma} \right|^\gamma \text{sgn} \left( \frac{dx_i}{d\sigma} \right) \int_{-\infty}^{\infty} \frac{du}{dy_i} \mathfrak{D}_{y_i}^\gamma u dy_i. \quad (12)$$

The result of equation (2.9) of [18] for regular diffusion is recovered upon substituting  $\gamma = 1$  in (12).

From (9),  $a$  decays exponentially at  $|y_i| \rightarrow \infty$ , and is localised near the centres  $x_i$  for  $i = 1, \dots, n$  of the spikes. In the outer region between the spikes,  $a$  is exponentially small. The inhibitor concentration is  $\mathcal{O}(1)$  across the domain when  $D \sim \mathcal{O}(1)$ . In the outer region expand  $h$  as

$$h \sim h^{(0)}(x, \sigma) + \mathcal{O}(\epsilon^\gamma), \quad \sigma = \epsilon^{\gamma+1} t.$$

Upon matching to the inner solution one obtains that

$$h^{(0)}(x_i, \sigma) = \bar{H}_i(\sigma), \quad \lim_{y_i \rightarrow \pm\infty} \frac{dH_i^{(1)}}{dy_i} = \lim_{\substack{y_i \rightarrow \pm\infty \\ \epsilon \rightarrow 0}} \epsilon^{-\gamma} \frac{\partial}{\partial y_i} \left( h(x_i + \epsilon^\gamma y_i, \sigma) - \bar{H}_i \right) = \lim_{x \rightarrow x_i^\pm} \frac{\partial h^{(0)}}{\partial x}. \quad (13)$$

To derive a differential equation for the outer problem for  $h^{(0)}$ , first note that the non-linear term in (2b) can be expressed as a linear combination of  $\delta$ -functions due to the localised behaviour of  $a$  as

$$\epsilon^{-\gamma} \frac{a^m}{h^s} = \sum_{i=1}^n b_i \delta(x - x_i), \quad (14)$$

where  $b_i$  is the weight of each spike given by

$$b_i = \epsilon^{-\gamma} \int_{x_i^-}^{x_i^+} \frac{a^m}{h^s} dx = \int_{-\infty}^{\infty} \frac{a^m}{h^s} dy_i \sim \bar{H}_i^{\beta m - s} \int_{-\infty}^{\infty} u^m dy_i.$$

Then, from (2b), the quasi-static outer equation for  $h^{(0)}$ , given by

$$Dh_{xx}^{(0)} - h^{(0)} = b_m \sum_{i=1}^n \bar{H}_i^{\beta m - s} \delta(x - x_i), \quad b_m \equiv \int_{-\infty}^{\infty} u^m dy, \quad (15)$$

is valid provided that the estimate  $\tau \epsilon^{\alpha \gamma} \partial_\sigma^\gamma h_0 \ll 1$  holds. Since  $\alpha = \gamma + 1$ , this condition holds when  $\tau$  satisfies  $\tau \sim o(\epsilon^{-(\gamma+1)\gamma})$ . This new threshold on  $\tau$  is stricter than that obtained above for neglecting the time derivative of the inhibitor in the inner region, and so this sets the condition on  $\tau$  as given in Principal result 2.1

The solution to (15) can be represented as

$$h^{(0)}(x, t) = b_m \sum_{i=1}^n \bar{H}_i^{\beta m - s} G(x; x_i),$$

where the Green's function  $G(x; x_i)$  satisfies (7b). Then

$$\lim_{y_i \rightarrow \infty} \partial_{y_i} H_i^{(1)} + \lim_{y_i \rightarrow -\infty} \partial_{y_i} H_i^{(1)} = \lim_{x \rightarrow x_i^+} h_x^{(0)} + \lim_{x \rightarrow x_i^-} h_x^{(0)} = 2b_m \left\{ \sum_{\substack{j=1 \\ j \neq i}}^n \bar{H}_j^{\beta m - s} G_x(x_i; x_j) + \bar{H}_i^{\beta m - s} \langle G_x(x_i; x_i) \rangle \right\}.$$

Substituting this result into the solvability condition (12) and combining with the matching condition (13) yields the desired differential-algebraic system.

**Remark 2.2** *As long as  $0 < \gamma < 1$ , the ODE in (7a) comprises two separate equations, governing the motion of the spikes according to  $\frac{dx_i}{d\sigma} \leq 0$ . For  $\gamma = 1$  the fractional operators in the definition of  $f(p; \gamma)$  approach  $\frac{d}{dy_i}$  regardless of  $\text{sgn}\left(\frac{dx_i}{d\sigma}\right)$ , and the fractional power on the left-hand side becomes unity, merging the two equations into a single equation for both the leftward and rightward motion of spikes.*

**Remark 2.3** *The temporal scale for the evolution of the spikes is  $\sigma = \epsilon^{\gamma+1} t$ , and, consequently, the motion of the spikes is slower under the effect of sub-diffusion than with regular diffusion. To see this, define  $\varepsilon = \epsilon^\gamma$  so that the activator diffusion coefficient is  $\varepsilon^2$ , and the spikes have speed  $\mathcal{O}(\varepsilon^{1+1/\gamma})$ . Since  $0 < \gamma < 1$  and  $1 + 1/\gamma > 2$ , this speed is slower than the speed  $\mathcal{O}(\varepsilon^2)$  found in [18] with regular diffusion.*

The DAE system in Principal result 2.1 can also be written in a vector form as

$$\mathbf{h} = b_m \mathcal{G} \mathbf{h}^{\gamma m - s}, \quad \frac{d^\gamma \mathbf{x}}{d\sigma} \sim -\frac{qb_m}{p+1} f(p; \gamma) \mathcal{H}^{-1} \mathcal{P} \mathbf{h}^{\beta m - s}, \quad (16)$$

$$d^\gamma \mathbf{x} / d\sigma \equiv (\text{sgn}(x'_1) |x'_1|^\gamma, \dots, \text{sgn}(x'_n) |x'_n|^\gamma)^T$$

with the matrices being

$$\mathcal{G} \equiv \begin{pmatrix} G(x_1; x_1) & \cdots & G(x_1; x_n) \\ \vdots & \ddots & \vdots \\ G(x_n; x_1) & \cdots & G(x_n; x_n) \end{pmatrix}, \quad \mathcal{H} \equiv \begin{pmatrix} \bar{H}_1 & 0 & \cdots & 0 \\ 0 & \ddots & \cdots & 0 \\ \vdots & \vdots & \ddots & \vdots \\ 0 & 0 & \cdots & \bar{H}_n \end{pmatrix}, \quad (17a)$$

and

$$\mathcal{P} \equiv \begin{pmatrix} \langle G_x(x_1; x_1) \rangle_1 & \cdots & G_x(x_1; x_n) \\ \vdots & \ddots & \vdots \\ G_x(x_n; x_1) & \cdots & \langle G_x(x_n; x_n) \rangle_n \end{pmatrix}, \quad \mathbf{h} \equiv \begin{pmatrix} \bar{H}_1 \\ \vdots \\ \bar{H}_n \end{pmatrix}, \quad \mathbf{h}^{\gamma^{m-s}} \equiv \begin{pmatrix} \bar{H}_1^{\beta^{m-s}} \\ \vdots \\ \bar{H}_n^{\beta^{m-s}} \end{pmatrix}. \quad (17b)$$

Similarly to the case of regular diffusion studied in [18], for  $n \geq 2$  this matrix DAE system is conveniently rewritten in terms of certain triadiagonal matrices. In Appendix A of [18] it was shown that

$$\mathcal{G} = \frac{\mathcal{B}^{-1}}{\sqrt{D}}, \quad (18)$$

where  $\mathcal{B}$  is the triadiagonal matrix

$$\mathcal{B} \equiv \begin{pmatrix} c_1 & d_1 & 0 & \cdots & 0 & 0 & 0 \\ d_1 & c_2 & \ddots & \ddots & \ddots & 0 & 0 \\ 0 & \ddots & \ddots & \ddots & \ddots & \ddots & 0 \\ \vdots & \ddots & \ddots & \ddots & \ddots & \ddots & \vdots \\ 0 & \ddots & \ddots & \ddots & \ddots & \ddots & 0 \\ 0 & 0 & \ddots & \ddots & \ddots & c_{n-1} & d_{n-1} \\ 0 & 0 & 0 & \cdots & 0 & d_{n-1} & c_n \end{pmatrix}, \quad (19a)$$

with matrix entries defined for  $n \geq 2$  in terms of  $x_i$  and  $\theta_o \equiv D^{-1/2}$  by

$$c_1 = \coth[\theta_o(x_2 - x_1)] + \tanh[\theta_o(1 + x_1)], \quad c_n = \coth[\theta_o(x_n - x_{n-1})] + \tanh[\theta_o(1 - x_n)], \quad (19b)$$

$$c_i = \coth[\theta_o(x_{i+1} - x_i)] + \coth[\theta_o(x_i - x_{i-1})], \quad i = 2, \dots, n-1, \quad (19c)$$

$$d_i = -\operatorname{csch}[\theta_o(x_{i+1} - x_i)], \quad i = 1, \dots, n-1. \quad (19d)$$

In addition, as shown in Appendix A of [18], the matrix product  $\mathcal{P}\mathcal{B}$  can also be written as a triadiagonal matrix of the form

$$\mathcal{P}\mathcal{B} \equiv \frac{1}{2D} \mathcal{P}_b, \quad \text{where} \quad \mathcal{P}_b \equiv \begin{pmatrix} e_1 & k_1 & 0 & \cdots & 0 & 0 & 0 \\ -k_1 & e_2 & \ddots & \ddots & \ddots & 0 & 0 \\ 0 & \ddots & \ddots & \ddots & \ddots & \ddots & 0 \\ \vdots & \ddots & \ddots & \ddots & \ddots & \ddots & \vdots \\ 0 & \ddots & \ddots & \ddots & \ddots & \ddots & 0 \\ 0 & 0 & \ddots & \ddots & \ddots & e_{n-1} & k_{n-1} \\ 0 & 0 & 0 & \cdots & 0 & -k_{n-1} & e_n \end{pmatrix}, \quad (20a)$$

with matrix entries defined for  $n \geq 2$  by

$$e_1 = \tanh[\theta_o(1+x_1)] - \coth[\theta_o(x_2-x_1)], \quad e_n = \coth[\theta_o(x_n-x_{n-1})] - \tanh[\theta_o(1-x_n)], \quad (20b)$$

$$e_i = \coth[\theta_o(x_i-x_{i-1})] - \coth[\theta_o(x_{i+1}-x_i)], \quad i = 2, \dots, n-1, \quad (20c)$$

$$k_i = \operatorname{csch}[\theta_o(x_{i+1}-x_i)], \quad i = 1, \dots, n-1. \quad (20d)$$

Substituting (18) into (16), the following result equivalent to that in (7a) is obtained.

**Corollary 2.1** *For  $n \geq 2$ , the DAE system in Principal result 2.1 is equivalent to the tridiagonal matrix DAE system*

$$\frac{d^\gamma \mathbf{x}}{d\sigma} \sim -\frac{q\theta_o}{2(p+1)} f(p; \gamma) \mathcal{H}^{-1} \mathcal{P}_b \mathbf{h}, \quad \mathcal{B} \mathbf{h} = b_m \theta_o \mathbf{h}^{\beta m - s}. \quad (21)$$

Here  $\frac{d^\gamma \mathbf{x}}{d\sigma}$  is defined in (16) and  $\mathcal{H}$ ,  $\mathcal{B}$ ,  $\mathcal{P}_b$  are defined in (17a), (19), and (20), respectively. For the case of one spike, i.e.  $n = 1$ , the motion of the centre of the spike is governed by

$$|x'_1|^\gamma \operatorname{sgn}(x'_1) \sim \frac{q\theta_o}{2(p+1)} f(p; \gamma) [\tanh(\theta_o(1-x_1)) - \tanh(\theta_o(1+x_1))]. \quad (22)$$

The explicit result in (22) was obtained by solving (7b) for  $G(x; x_1)$  and evaluating the required terms in the ODE for  $x_1$  in Principal result 2.1. The advantage of the formulation for  $n \geq 2$  in (21), as compared to that in Principal result 2.1, is that (21) is expressed only in terms of tridiagonal matrices.

The DAE system (21) has an equilibrium state with spikes of a common height. This state is the same as with regular diffusion and is characterised by a pattern of  $n$  spikes centred at  $x_i = -1 + (2i-1)/n$  for  $i = 1, \dots, n$ , with a common spike height  $\bar{H}$  given by

$$\bar{H} = \left( \frac{2}{b_m} \sqrt{\mu D} \tanh \frac{\theta_o}{n} \right)^{1/(\beta m - s - 1)}. \quad (23)$$

From (21), the dynamics of the spikes depends on the anomaly dependent factor  $f(p; \gamma)$ . Some key properties of  $f(p; \gamma)$  are derived in §2.1.

## 2.1 Properties of the anomaly dependent function $f(p; \gamma)$

The DAE system for spike evolution depends on the anomaly dependent factor  $f(p; \gamma)$  defined by

$$f(p; \gamma) = \left( \int_{-\infty}^{\infty} u^{p+1} dy \right) / \left( \int_{-\infty}^{\infty} u'(y) \mathfrak{D}_y^\gamma u dy \right). \quad (24)$$

To study the influence of  $\gamma$  in  $f(p; \gamma)$  the fractional operator  $\mathfrak{D}_y^\gamma u$  must be first computed. For the numerical computation below the fractional operator in Lemma 2.1 was truncated as

$$\mathfrak{D}_y^\gamma u(y) = \frac{1}{\Gamma(-\gamma)} \operatorname{sgn} \left( \frac{dx_i}{d\sigma} \right) \int_0^{y_\infty} \left\{ u(y) - u \left( y + \operatorname{sgn} \left( \frac{dx_i}{d\sigma} \right) \zeta \right) \right\} \frac{d\zeta}{\zeta^{\gamma+1}}, \quad (25)$$

where  $y_\infty$  is a large positive number. Since  $u$  is an even function, it is readily observed that

$$\mathfrak{D}_{(-y)}^\gamma u(-y) \Big|_{x'_i > 0} = -\mathfrak{D}_y^\gamma u(y) \Big|_{x'_i < 0}.$$

Thus, it suffices to compute the operator for  $x'_i < 0$ . Using this property together with the fact that  $u$  is even, it follows immediately that

$$\int_{-\infty}^{\infty} u'(y) \mathfrak{D}_y^\gamma u(y) \Big|_{x'_i > 0} dy = - \int_{-\infty}^{\infty} u'(y) \mathfrak{D}_{(-y)}^\gamma u(-y) \Big|_{x'_i < 0} dy = \int_{-\infty}^{\infty} u'(\tilde{y}) \mathfrak{D}_{\tilde{y}}^\gamma u(\tilde{y}) \Big|_{x'_i < 0} d\tilde{y}.$$

From the definition of  $f(p; \gamma)$  in (24) it is concluded that

$$f(p; \gamma) \Big|_{x'_i > 0} = f(p; \gamma) \Big|_{x'_i < 0} \quad \forall p, \gamma.$$

Thus, the anomaly factor does not depend on the sign of  $x'_i$ .

For a straightforward numerical computation, the expression (25) was regularised using integration by parts twice to get

$$\begin{aligned} \mathfrak{D}_y^\gamma u(y) &= \frac{y_\infty^{-\gamma}}{\Gamma(1-\gamma)} \operatorname{sgn} x'_i \left( u(y) - u(y + y_\infty \operatorname{sgn} x'_i) \right) + \frac{y_\infty^{1-\gamma}}{\Gamma(2-\gamma)} u'(y + y_\infty \operatorname{sgn} x'_i) \\ &\quad - \frac{1}{\Gamma(2-\gamma)} \int_y^{y+y_\infty \operatorname{sgn} x'_i} (u(\xi) - u^p(\xi)) \left( (\xi - y) \operatorname{sgn} x'_i \right)^{1-\gamma} d\xi. \end{aligned} \quad (26)$$

In the limit  $\gamma \rightarrow 1$  it is possible to integrate the last term in this expression and then pass to the limit to obtain

$$\lim_{\gamma \rightarrow 1^-} \mathfrak{D}_y^\gamma u = \lim_{y_\infty \rightarrow \infty} \left\{ \frac{\operatorname{sgn} x'_i}{y_\infty} \left( u(y) - u(y + y_\infty \operatorname{sgn} x'_i) \right) + u'(y + y_\infty \operatorname{sgn} x'_i) - \int_y^{y+y_\infty \operatorname{sgn} x'_i} u''(\xi) d\xi \right\},$$

which yields  $\lim_{\gamma \rightarrow 1^-} \mathfrak{D}_y^\gamma u = u'(y)$ . This shows that as  $\gamma \rightarrow 1^-$  the fractional operator for both signs of  $x'_i$  recovers the first integer derivative  $u'$ , which is an odd function.

With (26) it is possible to compute the fractional derivative analytically at the stagnation limit  $\gamma = 0$ . For any fixed  $y_\infty \neq 0$

$$\begin{aligned} \lim_{\gamma \rightarrow 0^+} \mathfrak{D}_y^\gamma u &= \operatorname{sgn} x'_i \left( u(y) - u(y + y_\infty \operatorname{sgn} x'_i) \right) + y_\infty u'(y + y_\infty \operatorname{sgn} x'_i) \\ &\quad - \int_y^{y+y_\infty \operatorname{sgn} x'_i} \left( (\xi - y) \operatorname{sgn} x'_i \right) u''(\xi) d\xi = 0. \end{aligned}$$

Thus  $\lim_{\gamma \rightarrow 0^+} \mathfrak{D}_y^\gamma u = 0$ , implying that  $f(p; \gamma) \rightarrow \infty$  as  $\gamma \rightarrow 0^+$ . To compute the asymptotics of  $f(p; \gamma)$  for  $0 < \gamma \ll 1$  use (26) with  $x'_i > 0$  to get

$$\mathfrak{D}_y^\gamma u(y) \Big|_{x'_i > 0} = \frac{u(y) - u(y + y_\infty)}{y_\infty^\gamma \Gamma(1-\gamma)} + \frac{y_\infty^{1-\gamma}}{\Gamma(2-\gamma)} u'(y + y_\infty) - \frac{1}{\Gamma(2-\gamma)} \int_y^{y+y_\infty} u''(\xi) (\xi - y)^{1-\gamma} d\xi.$$

For  $\gamma \ll 1$  expand using

$$\Gamma(2-\gamma) = 1 - \gamma \Gamma'(2) + \mathcal{O}(\gamma^2), \quad \Gamma(1-\gamma) \sim 1 + \gamma(1 - \Gamma'(2)) + \mathcal{O}(\gamma^2), \quad y_\infty^{-\gamma} \sim 1 - \gamma \ln y_\infty + \mathcal{O}(\gamma^2).$$

After some algebra one obtains that for any fixed  $y_\infty \neq 0$

$$\lim_{\gamma \rightarrow 0^+} \mathfrak{D}_y^\gamma u = \gamma \left\{ \left( u(y) - u(y + y_\infty) \right) (\ln y_\infty - 1) - u'(y + y_\infty) y_\infty \ln y_\infty + \int_y^{y+y_\infty} u''(\xi) (\xi - y) \ln(\xi - y) d\xi \right\} + \mathcal{O}(\gamma^2).$$

Note that in this expression the term of order  $\mathcal{O}(\gamma)$  is not uniformly bounded as  $y_\infty \rightarrow \infty$ . This shows that the limiting procedures  $\gamma \rightarrow 0^+$  and  $y_\infty \rightarrow \infty$  do not commute.

In figure 1  $\mathfrak{D}_y^\gamma u$  is plotted with  $x'_i < 0$  for  $p = 2$  and a range of values of  $\gamma$ . In the computation the integration parameter  $y_\infty = 5$  and integration step  $\delta\xi = 0.05$  were used. As a check on the computation, the numerical results were shown to agree very well with the analytical result  $\mathfrak{D}_y u = u'$  when  $\gamma = 1$  (not shown). The function  $f(p; \gamma)$  was computed numerically and is shown as a surface in the  $(p, \gamma)$  parameter

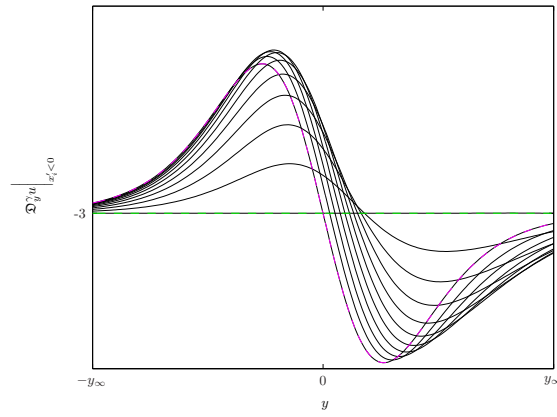


Figure 1: Numerical computation of  $\mathfrak{D}_y^\gamma u|_{x'_i < 0}$  for  $\gamma$  equally spaced between  $\gamma = 0$  ( stagnation ) and  $\gamma = 1$  ( regular diffusion ). The dashed horizontal line corresponds to the stagnation limit  $\gamma = 0$ , while the dashed curve corresponds to the regular diffusion limit  $\mathfrak{D}_y u = u'(y)$ , which is an odd function. The fractional derivatives for  $0 < \gamma < 1$  are neither odd nor even.

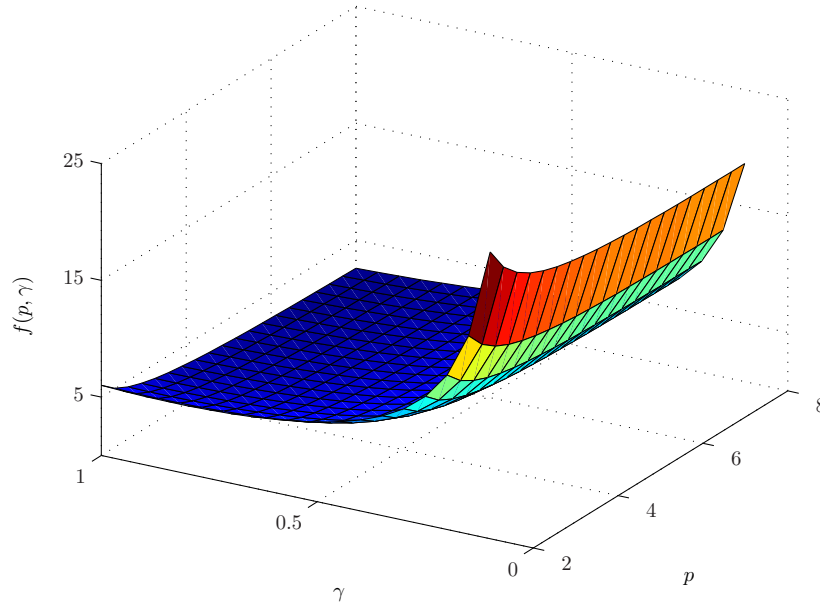


Figure 2: The anomaly dependent function  $f(p; \gamma)$

plane in figure 2. In figure 3  $f(p; \gamma)$  is plotted for fixed values of  $p$ . Notice that the curve  $f(2; \gamma)$  is not monotone. At  $p = 3$  the minimum is obtained when  $\gamma$  is very close to  $\gamma = 1$ . For  $p > 3$  the curves appear to be monotone. For  $\gamma = 1$  an exact expression is known from [18]

$$f(p; 1) = 2 \left( \frac{p+1}{p-1} \right).$$

Thus,  $f(p; 1)$  is a monotonously decreasing function of  $p$  with a limiting value  $\lim_{p \rightarrow \infty} f(p; 1) = 2$ . In summary, the numerical results in this sub-section support the conjecture that  $f(p; \gamma) > 0$  for all  $0 < \gamma < 1$  and  $p > 1$ . Such a result is needed below to classify the stability properties of the equilibrium of the DAE system in Corollary 2.1.

## 2.2 Evolution of a two-spike pattern

For a quasi-equilibrium pattern of two spikes centred at  $x_1$  and  $x_2$ , so that  $-1 < x_1(\sigma) < x_2(\sigma) < 1$ , the non-linear DAE system in (21) of Corollary 2.1 for the spike motion can readily be simplified to the following

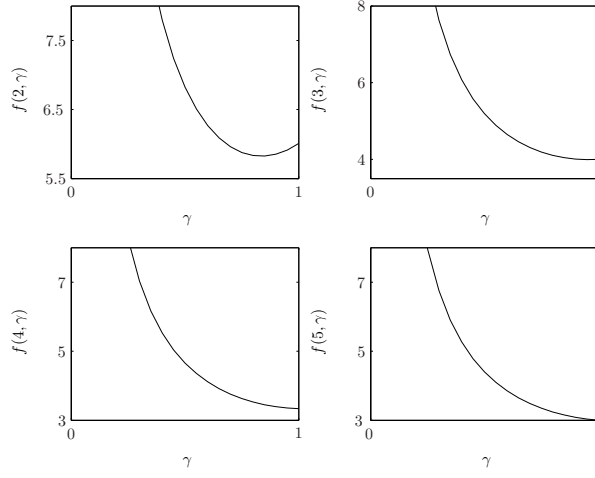


Figure 3: The function  $f(p; \gamma)$  for  $p = 2, 3, 4, 5$ .

result.

**Corollary 2.2** For  $n = 2$  the DAE system for the spike evolution is given by

$$\frac{d^\gamma x_1}{d\sigma} = -\frac{q\theta_o f(p; \gamma)}{2(p+1)} (\tanh[\theta_o(1+x_1)] - \coth[\theta_o(x_2-x_1)] + \zeta_H^{-1} \operatorname{csch}[\theta_o(x_2-x_1)]) \quad (27a)$$

$$\frac{d^\gamma x_2}{d\sigma} = -\frac{q\theta_o f(p; \gamma)}{2(p+1)} (-\zeta_H \operatorname{csch}[\theta_o(x_2-x_1)] + \coth[\theta_o(x_2-x_1)] - \tanh[\theta_o(1-x_2)]) . \quad (27b)$$

Here  $\zeta_H \equiv \bar{H}_1/\bar{H}_2$  is the ratio of spike heights, and satisfies the non-linear algebraic equation  $\mathcal{F}(\zeta_H) = 0$ , where  $\mathcal{F}(\zeta_H)$  is defined by

$$\begin{aligned} \mathcal{F}(\zeta_H) \equiv & \operatorname{csch}(\theta_o(x_2-x_1)) \left( \zeta_H^{\beta m-s+1} - 1 \right) + \coth(\theta_o(x_2-x_1)) \left( \zeta_H - \zeta_H^{\beta m-s} \right) \\ & + \tanh(\theta_o(1+x_1)) \zeta_H - \tanh(\theta_o(1-x_2)) \zeta_H^{\beta m-s} . \end{aligned} \quad (27c)$$

For the special case of a symmetric two-spike quasi-equilibrium solution for which  $x_1 = -x_2$  at all times, the spikes have equal height so that  $\zeta = 1$ . For this special case the ODE's in (27) reduce to

$$\frac{d^\gamma \mathbf{x}}{d\sigma} = -\frac{q\theta_o f(p; \gamma)}{2(p+1)} \left\{ \tanh(\theta_o(1-x_2)) - \tanh(\theta_o x_2) \right\} \begin{pmatrix} 1 \\ -1 \end{pmatrix} . \quad (28)$$

In terms of the instantaneous spike location  $x_2 = x_2(\sigma)$ , the common spike height  $\bar{H}$  is given by

$$\bar{H} = \left( \frac{\tanh(\theta_o x_2) + \tanh(\theta_o(1-x_2))}{b_m \theta_o} \right)^{1/(\beta m-s-1)} .$$

The qualitative feature of the dynamics under (28) is readily apparent. Suppose that  $0 < x_2(0) < 1/2$  and  $x_1(0) = -x_2(0)$ . Then,  $x_2' = -x_1' > 0$  for all  $\sigma$ , and  $x_2(\sigma)$  satisfies the ODE

$$|x_2'|^\gamma = \frac{q\theta_o f(p; \gamma)}{2(p+1)} \left\{ \tanh(\theta_o(1-x_2)) - \tanh(\theta_o x_2) \right\} . \quad (29)$$

Since  $f(p; \gamma) > 0$ ,  $x_2 \rightarrow 1/2^-$  as  $\sigma \rightarrow \infty$ . In a similar way, if  $1/2 < x_2(0) < 1$ , then  $x_2' = -x_1' < 0$  and  $x_2 \rightarrow 1/2^+$  as  $\sigma \rightarrow \infty$ .

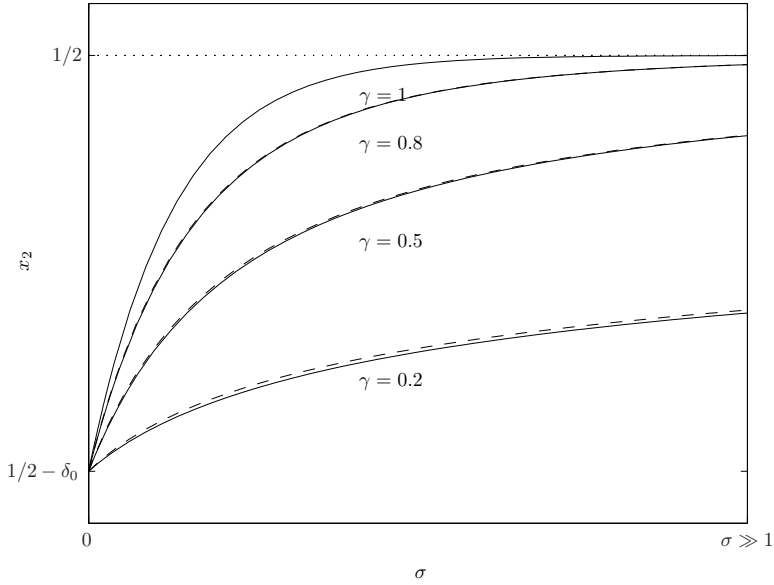


Figure 4: Evolution of two symmetric spikes ( only the rightmost spike shown ) for several values of  $\gamma$ : full numerical from (29) ( solid ) and approximate solution from (30) ( dashed ). Note the slow algebraic decay of the initial disturbance  $\delta_0$  as opposed to the exponential decay for the case  $\gamma = 1$ . The system parameters used are  $\delta_0 = 0.4$ ,  $p = 2$ ,  $q = 1$ , and  $D = 1$ .

Apart from the different time scales of spike motion, another key effect of sub-diffusion is that the approach of a spike to its equilibrium state is algebraic in  $\sigma$ . This is in contrast to the exponential rate of approach as typical for the case of regular diffusion. Setting  $x_2 = 1/2 - \delta$  with  $\delta \rightarrow 0^+$  in (29) one obtains upon linearisation that  $\delta$  satisfies

$$\delta' \sim -\mu \delta^{1/\gamma}, \quad \mu \equiv \left( \frac{qf(p; \gamma)}{(p+1)D} \operatorname{sech}^2 \frac{\theta_o}{2} \right)^{1/\gamma}.$$

With the initial value  $\delta(0) = \delta_0$  the solution to this ODE is

$$\delta \sim \left( \delta_0^{(\gamma-1)/\gamma} + \frac{\mu(1-\gamma)\sigma}{\gamma} \right)^{-\gamma/(1-\gamma)}. \quad (30)$$

Therefore, for  $\sigma \gg 1$ , the algebraic approach to the equilibrium is governed by  $\delta \sim c \sigma^{-\gamma/(1-\gamma)}$ , where  $c$  is some positive constant. Figure 4 compares the sub-diffusive motion for several values of  $\gamma$  to that of regular spike motion with  $\gamma = 1$ .

### 3 Stability theory for exponential disturbances

The uniformly valid approximation of the quasi-equilibrium profile on  $-1 < x < 1$  constructed in §2 has the form

$$a \sim a_{qe} = \sum_{i=1}^n \bar{H}_i^\beta(\sigma) u \left( \frac{x - x_i}{\epsilon^\gamma} \right), \quad h \sim h_{qe} = b_m \sum_{i=1}^n \bar{H}_i^{\beta m - s}(\sigma) G(x; x_i). \quad (31)$$

For the study of stability properties the slow time variable  $\sigma$  is considered fixed and satisfies  $\sigma = \mathcal{O}(1)$ , so that  $t \sim \mathcal{O}(\epsilon^{-(\gamma+1)}) \gg 1$ . In the context of fractional differential equations the perturbations do not grow exponentially in time with a constant growth rate, depriving the eigenvalue problem of its classical meaning. Instead, it should be regarded as an asymptotic theory of perturbations that evolve exponentially in time to leading order:

$$a \sim a_{qe} + e^{\lambda t} \tilde{a}(x), \quad \tilde{a}(x) \sim \tilde{a}^{(0)} + \epsilon^\gamma \tilde{a}^{(1)} + \dots, \quad |\tilde{a}| \ll 1, \quad (32a)$$

$$h \sim h_{qe} + e^{\lambda t} \tilde{h}(x), \quad \tilde{h}(x) \sim \tilde{h}^{(0)} + \epsilon^\gamma \tilde{h}^{(1)} + \dots, \quad |\tilde{h}| \ll 1, \quad (32b)$$

$$\lambda(t) \sim \lambda^{(0)} + \epsilon^\gamma \lambda^{(1)}(t) + \dots, \quad \lambda^{(0)} = \text{const.}$$

Hereinafter  $\{\lambda^{(0)}, \tilde{a}^{(0)}\}$  are referred to as eigenvalue and eigenfunction for convenience, yet one must bear in mind that only at the limit  $\gamma = 1$  do they in fact correspond to these classical notions. When substituting (32) into (2) and collecting the leading order terms, the following expression involving the fractional derivative of the exponent appears:

$$\mathcal{S} \equiv e^{-\lambda^{(0)}t} \frac{d^\gamma}{dt^\gamma} e^{\lambda^{(0)}t} = -\frac{1}{\Gamma(-\gamma)} \int_0^t \frac{1 - e^{-\lambda^{(0)}\zeta}}{\zeta^{\gamma+1}} d\zeta. \quad (33)$$

In the limit  $t \rightarrow \infty$  the integral converges if and only if  $\Re\lambda^{(0)} \geq 0$ , which is quite different from the behaviour with an integer derivative. With  $\gamma = 1$  and  $\lambda^{(0)} > 0$  the derivative  $\frac{d}{dt} e^{\lambda^{(0)}t}$  diverges exponentially at  $t \rightarrow \infty$ , and then the factor  $\exp(-\lambda^{(0)}t)$  makes the expression finite. With  $\gamma = 1$  and  $\lambda^{(0)} < 0$  the factor  $\exp(-\lambda^{(0)}t)$  diverges exponentially, but the derivative  $\frac{d}{dt} e^{\lambda^{(0)}t}$  decays exponentially, again resulting in a finite expression. In the sub-diffusive case with  $0 < \gamma < 1$  and  $\lambda^{(0)} > 0$  the derivative  $\frac{d^\gamma}{dt^\gamma} e^{\lambda^{(0)}t}$  diverges exponentially at  $t \rightarrow \infty$ , and the factor  $\exp(-\lambda^{(0)}t)$  makes the expression finite. However for  $\lambda^{(0)} < 0$  the derivative  $\frac{d^\gamma}{dt^\gamma} e^{\lambda^{(0)}t}$  decays only algebraically, and with the exponential factor  $\exp(-\lambda^{(0)}t)$  the expression is divergent. Therefore the derivation below is valid for  $\Re\lambda^{(0)} \geq 0$ . This nuance adds a certain subtlety to the interpretation of the current stability theory, rendering it sufficient to study the onset of instability, i.e. the limit  $\Re\lambda^{(0)} \rightarrow 0^+$ , yet it is impossible to trace eigenvalues in the left half of the complex plane. This is summarised in the following lemma.

**Lemma 3.1** *In the limit  $t = \sigma\epsilon^{-(\gamma+1)} \gg 1$  with  $\epsilon \rightarrow 0$  and  $\sigma \sim \mathcal{O}(1)$  the asymptotic relation*

$$\mathcal{S} \equiv e^{-\lambda^{(0)}t} \frac{d^\gamma}{dt^\gamma} e^{\lambda^{(0)}t} \sim \lambda^{(0)\gamma} + \mathcal{O}\left(\epsilon^{\gamma(\gamma+1)}\right),$$

*holds if and only if  $\Re\lambda^{(0)} \geq 0$ .*

**PROOF** Integrate the expression in (33) by parts and let  $t = \mathcal{O}(\epsilon^{-(\gamma+1)}) \gg 1$  to obtain

$$\begin{aligned} \lim_{\epsilon \rightarrow 0} e^{-\lambda^{(0)}t} \frac{d^\gamma}{dt^\gamma} e^{\lambda^{(0)}t} &= -\frac{1}{\Gamma(1-\gamma)} \lim_{\epsilon \rightarrow 0} \left\{ \frac{1 - e^{-\lambda^{(0)}t}}{t^\gamma} - \lambda^{(0)} \int_0^t e^{-\lambda^{(0)}\zeta} \zeta^{-\gamma} d\zeta \right\} \sim \\ &\frac{\lambda^{(0)\gamma}}{\Gamma(1-\gamma)} \lim_{\epsilon \rightarrow 0} \int_0^{\lambda^{(0)}t} e^{-\xi} \xi^{-\gamma} d\xi + \mathcal{O}\left(\epsilon^{\gamma(\gamma+1)}\right). \end{aligned}$$

The error order in this expression arises from the algebraic decay of  $t^{-\gamma}$  regardless of the exact value of  $\lambda^{(0)}$ . Notice also that the path of integration of the last integral above is a line in the complex plane. To evaluate the integral, form a closed contour consisting of this line, an arc of radius  $R \equiv |\lambda^{(0)}|t$  (corresponding to  $R \rightarrow \infty$  at the limit  $\epsilon \rightarrow 0$ ), the interval  $(\epsilon, R)$  on the real axis and an arc of radius  $\epsilon \rightarrow 0$  ( $\epsilon$  is independent of  $\epsilon$ ). The contour is depicted in figure 5. Upon using the residue theorem one gets

$$\begin{aligned} \lim_{\epsilon \rightarrow 0} e^{-\lambda^{(0)}t} \frac{d^\gamma}{dt^\gamma} e^{\lambda^{(0)}t} &= \frac{\lambda^{(0)\gamma}}{\Gamma(1-\gamma)} \lim_{\substack{R \rightarrow \infty \\ \epsilon \rightarrow 0}} \left\{ iR^{1-\gamma} \int_0^{\arg \lambda^{(0)}} e^{-Re^{i\theta}} e^{i(1-\gamma)\theta} d\theta \right. \\ &\left. - i\epsilon^{1-\gamma} \int_0^{\arg \lambda^{(0)}} e^{-\epsilon e^{i\theta}} e^{i(1-\gamma)\theta} d\theta + \int_\epsilon^R e^{-\xi} \xi^{-\gamma} d\xi \right\} \sim \lambda^{(0)\gamma} + \mathcal{O}\left(\epsilon^{\gamma(\gamma+1)}\right), \end{aligned}$$

where the first integral exists if and only if  $\Re\lambda^{(0)} \geq 0$ . ■

**Remark 3.1** *Since  $\gamma < \gamma(\gamma + 1)$  for any  $0 < \gamma \leq 1$ , the asymptotic estimate above for the time scale  $t = \mathcal{O}(\epsilon^{-(\gamma+1)})$  shows that  $\mathcal{S} \sim \lambda^{(0)\gamma}$  provided that  $\lambda^{(0)}$  satisfies  $\Re\lambda^{(0)} > 0$  and is not too close to the origin in the sense that  $|\lambda^{(0)}|$  must satisfy  $|\lambda^{(0)}| \sim \mathcal{O}(\epsilon)$  or larger.*

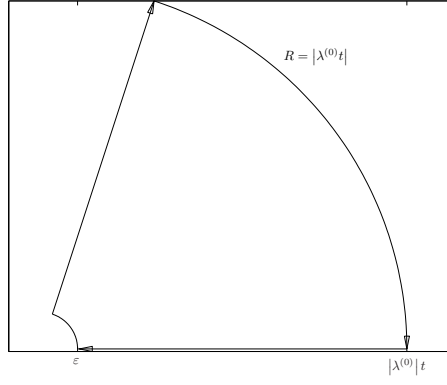


Figure 5: Closed integration contour in the evaluation of  $e^{-\lambda^{(0)} t} \frac{d^\gamma}{dt^\gamma} e^{\lambda^{(0)} t}$

### 3.1 The nonlocal eigenvalue problem

With Lemma 3.1 the linearisation around the quasi-equilibrium pattern (31) is

$$\lambda^{(0)\gamma} \tilde{a}^{(0)} = \left( \epsilon^{2\gamma} \frac{d^2}{dx^2} - 1 + p \frac{a_{qe}^{p-1}}{h_{qe}^q} \right) \tilde{a}^{(0)} - q \frac{a_{qe}^p}{h_{qe}^{q+1}} \tilde{h}^{(0)}, \quad (34a)$$

$$\tau \lambda^{(0)\gamma} \tilde{h}^{(0)} = \left( D \frac{d^2}{dx^2} - 1 - \epsilon^{-\gamma} s \frac{a_{qe}^m}{h_{qe}^{s+1}} \right) \tilde{h}^{(0)} + \epsilon^{-\gamma} m \frac{a_{qe}^{m-1}}{h_{qe}^s} \tilde{a}^{(0)}, \quad (34b)$$

$$\frac{d}{dx} \tilde{a}^{(0)} \Big|_{x=\pm 1} = \frac{d}{dx} \tilde{h}^{(0)} \Big|_{x=\pm 1} = 0. \quad (34c)$$

A localised eigenfunction of form

$$\tilde{a}^{(0)} \sim \sum_{i=1}^n \tilde{a}_i^{(0)} \left( \frac{x - x_i}{\epsilon^\gamma} \right) \quad (35)$$

is expected. In the outer region away from the spikes one can represent (34b) as ( see the derivation of Proposition 2.3 of [20] )

$$D \frac{d^2}{dx^2} \tilde{h}^{(0)} - \left( 1 + \tau \lambda^{(0)\gamma} + sb_m \sum_{i=1}^n \bar{H}_i^{\beta m - s - 1} \delta(x - x_i) \right) \tilde{h}^{(0)} = - \sum_{i=1}^n w_i \delta(x - x_i), \quad (36)$$

$$w_i = m \bar{H}_i^{\beta m - s - \beta} \int_{-\infty}^{\infty} u^{m-1} \tilde{a}_i^{(0)} dy_i.$$

Problem (36) with boundary conditions (34c) is equivalent to the following problem defined on  $[-1, 1]$ , which has internal continuity and jump conditions:

$$D \frac{d^2}{dx^2} \tilde{h}^{(0)} - \left( 1 + \tau \lambda^{(0)\gamma} \right) \tilde{h}^{(0)} = 0,$$

$$\tilde{h}^{(0)}(x_i^+) = \tilde{h}^{(0)}(x_i^-), \quad i = 1, \dots, n,$$

$$D \left( \frac{d}{dx} \tilde{h}^{(0)} \Big|_{x_i^+} - \frac{d}{dx} \tilde{h}^{(0)} \Big|_{x_i^-} \right) = sb_m \bar{H}_i^{\beta m - s - 1} \tilde{h}^{(0)}(x_i) - w_i, \quad i = 1, \dots, n, \quad (37a)$$

$$\frac{d}{dx} \tilde{h}^{(0)} \Big|_{x=\pm 1} = 0.$$

This problem is readily solved by patching together appropriate solutions defined on each sub-interval. Upon substituting (35) into (34a), one obtains  $n$  separate problems, one in the vicinity of each spike:

$$\frac{d^2}{dy_i^2} \tilde{a}_i^{(0)} - \left( 1 + \lambda^{(0)\gamma} - pu^{p-1} \right) \tilde{a}_i^{(0)} = q \bar{H}_i^{\beta-1} u^p(y_i) \tilde{h}^{(0)}(x_i), \quad \lim_{|y_i| \rightarrow \infty} \tilde{a}_i^{(0)} = 0, \quad i = 1, \dots, n.$$

For the case of  $n$ -identical spikes, the following result is analogous to Proposition 2.3 of [20].

**Proposition 3.1** *For an equilibrium  $n$ -spike pattern with spikes of equal height the localised eigenfunction corresponding to the activator concentration satisfies the non-local fractional eigenvalue problem*

$$\left(\frac{d^2}{dy^2} - 1 + pu^{p-1}\right) \tilde{A}^{(0)} - \chi_i u^p \frac{\int_{-\infty}^{\infty} u^{m-1} \tilde{A}^{(0)} dy}{\int_{-\infty}^{\infty} u^m dy} = \lambda^{(0)\gamma} \tilde{A}^{(0)}, \quad -\infty < y < \infty, \quad (38a)$$

$$\lim_{|y| \rightarrow \infty} \tilde{A}^{(0)} = 0. \quad (38b)$$

In this NLEP there are  $n$  choices for the multiplier  $\chi_i$ , given by

$$\chi_i \equiv qm \left( s + \frac{\kappa_i \theta}{2 \theta_o} \coth \frac{\theta_o}{n} \right)^{-1}, \quad \theta \equiv \theta_o \sqrt{1 + \tau \lambda^{(0)\gamma}}, \quad \theta_o \equiv D^{-1/2}, \quad (38c)$$

$$\kappa_i \equiv \kappa \left( (\lambda^{(0)\gamma}; n, i) \right) = 2 \operatorname{csch} \frac{2\theta}{n} \left\{ \cosh \left( \frac{2\theta}{n} \right) - \cos \left( \frac{\pi(i-1)}{n} \right) \right\}, \quad i = 1, \dots, n.$$

PROOF Upon seeking a common ( up to a scalar ) localised eigenfunction for all  $n$  spikes, the general form (35) simplifies to

$$\tilde{a}^{(0)} \sim \sum_{i=1}^n c_i \tilde{A}^{(0)} \left( \frac{x - x_i}{\epsilon^\gamma} \right), \quad (39)$$

where the constants  $c_i$  for  $i = 1, \dots, n$  are as determined below. Then, by using (23) and rescaling the equations (37) with  $\tilde{h}^{(0)} \mapsto \tilde{H} \tilde{h}^{(0)}$  and  $\tilde{A}^{(0)} \mapsto \tilde{H}^\beta \tilde{A}^{(0)}$ , one obtains

$$D \frac{d^2}{dx^2} \tilde{h}^{(0)} - \left( 1 + \tau \lambda^{(0)\gamma} \right) \tilde{h}^{(0)} = 0, \quad -1 < x < 1, \quad (40a)$$

$$\tilde{h}^{(0)}(x_i^+) = \tilde{h}^{(0)}(x_i^-), \quad \left. \frac{d}{dx} \tilde{h}^{(0)} \right|_{x=\pm 1} = 0,$$

$$\left. \frac{d}{dx} \tilde{h}^{(0)} \right|_{x_i^+} - \left. \frac{d}{dx} \tilde{h}^{(0)} \right|_{x_i^-} = 2\theta_o \tanh \left( \frac{\theta_o}{n} \right) \left( s \tilde{h}^{(0)}(x_i) - \frac{m}{b_m} c_i \int_{-\infty}^{\infty} u^{m-1} \tilde{A}^{(0)} dy \right), \quad (40b)$$

$$\left\{ \frac{d^2}{dy^2} \tilde{A}^{(0)} - \left( 1 + \lambda^{(0)\gamma} - pu^{p-1} \right) \tilde{A}^{(0)} \right\} c_i = qu^p \tilde{h}^{(0)}(x_i), \quad \lim_{|y| \rightarrow \infty} \tilde{A}^{(0)} = 0.$$

Next, (40a) is solved for  $\tilde{h}^{(0)}$  on each sub-interval to obtain

$$\tilde{h}^{(0)} = \begin{cases} \tilde{h}^{(0)}(x_1) \frac{\cosh(\theta(x+1))}{\cosh(\theta(x_1+1))} & -1 < x < x_1 \\ \tilde{h}^{(0)}(x_{i+1}) \frac{\sinh(\theta(x-x_i))}{\sinh(2\theta/n)} + \tilde{h}^{(0)}(x_i) \frac{\sinh(\theta(x-x_{i+1}))}{\sinh(2\theta/n)} & x_i < x < x_{i+1} \\ \tilde{h}^{(0)}(x_n) \frac{\cosh(\theta(x-1))}{\cosh(\theta(x_n-1))} & x_n < x < 1, \end{cases} \quad \begin{matrix} \\ i=1, \dots, n-1 \end{matrix}$$

where the continuity constraints for  $\tilde{h}^{(0)}$  at each  $x_i$  were imposed. To determine  $\tilde{h}^{(0)}(x_i)$  the internal jump conditions for  $\frac{d}{dx} \tilde{h}^{(0)}$  at each  $x_i$  must be satisfied. Thus the tridiagonal matrix system is obtained

$$\left( B + 2s \frac{\theta_o}{\theta} \tanh \left( \frac{\theta_o}{n} \right) I \right) \mathbf{h}^{(0)} = 2 \frac{\theta_o}{\theta} \tanh \left( \frac{\theta_o}{n} \right) \frac{m}{b_m} \mathbf{c} \int_{-\infty}^{\infty} u^{m-1} \tilde{A}^{(0)} dy, \quad (41)$$

where  $\mathbf{I}$  is the  $n \times n$  identity matrix, and the matrix  $\mathbf{B}$  is defined by

$$\mathbf{B} \stackrel{\text{def}}{=} \begin{pmatrix} d_\lambda & f_\lambda & 0 & \dots & \dots & 0 \\ f_\lambda & e_\lambda & f_\lambda & 0 & \dots & 0 \\ 0 & f_\lambda & e_\lambda & f_\lambda & \dots & 0 \\ \vdots & \vdots & \ddots & \ddots & \vdots & \vdots \\ 0 & \dots & f_\lambda & e_\lambda & f_\lambda & 0 \\ 0 & \dots & 0 & f_\lambda & e_\lambda & f_\lambda \\ 0 & \dots & \dots & 0 & d_\lambda & f_\lambda \end{pmatrix}, \quad \begin{aligned} d_\lambda &= \coth\left(\frac{2\theta}{n}\right) + \tanh\left(\frac{\theta}{n}\right), \\ e_\lambda &= 2 \coth\left(\frac{2\theta}{n}\right), \\ f_\lambda &= -\operatorname{csch}\left(\frac{2\theta}{n}\right), \end{aligned}$$

$$\left(\mathbf{h}^{(0)}\right)_i = \tilde{h}^{(0)}(x_i), \quad (\mathbf{c})_i = c_i.$$

The eigenvectors of  $\mathbf{B}$  are readily determined as

$$\mathbf{c}_i^\top = \left\{ \cos \frac{\pi(i-1)}{2n}, \cos \frac{3\pi(i-1)}{2n}, \dots, \cos \left( \left( n - \frac{1}{2} \right) \frac{\pi(i-1)}{n} \right) \right\}, \quad i = 1, \dots, n, \quad (42)$$

with corresponding eigenvalue

$$\kappa_i \equiv \kappa \left( (\lambda^{(0)})^\gamma; n, i \right) = 2 \operatorname{csch} \frac{2\theta}{n} \left( \cosh \frac{2\theta}{n} - \cos \frac{\pi(i-1)}{n} \right) \geq 0, \quad i = 1, \dots, n.$$

The coefficients  $c_i$  for  $i = 1, \dots, n$  in (39) are the components of any one of the eigenvectors in (42). Any eigenpair  $\{\kappa, \mathbf{c}\}$  satisfying  $\mathbf{B}\mathbf{c} = \nu \mathbf{c}$  also satisfies  $(\mathbf{B} + \alpha\mathbf{I})\mathbf{c} = (\nu + \alpha)\mathbf{c}$  for all  $\alpha$ . Therefore, by taking  $\alpha = 2s \frac{\theta_o}{\theta} \tanh \frac{\theta_o}{n}$ , the inversion of (41) and substitution of  $\mathbf{h}^{(0)}$  into (40b) complete the proof.  $\blacksquare$

**Remark 3.2** *The eigenpairs  $\{\kappa_i, \mathbf{c}_i\}$  for  $i = 1, \dots, n$ , are identical to those computed for regular diffusion. The mode  $i = 1$  is called the synchronous mode, since the corresponding eigenfunction governing the instability in the spike amplitudes is  $\mathbf{c}_1 = (1, \dots, 1)^t$ . The other modes, for  $1 < i \leq n$  are called asynchronous or competition modes since, by the symmetric nature of the matrix  $\mathbf{B}$ , they satisfy  $\mathbf{c}_i \cdot (1, \dots, 1)^t = 0$ . Substitution of  $\gamma = 1$  in (38) recovers the problem corresponding to regular diffusion. Moreover, the normal problem can be obtained by the mapping  $\lambda^{(0)\gamma} \mapsto \lambda^{(0)}$ . Hence the stability theorems for the normal case can be applied directly to infer the location of  $\Re\lambda^{(0)\gamma}$  and thus the location of  $\Re\lambda^{(0)}$ .*

The NLEP associated with regular diffusion ( $\gamma = 1$ ) is referred to as the *regular* NLEP. This spectral problem is given by (38) where  $\lambda^{(0)\gamma}$  is replaced by the eigenvalue  $\nu$ . In [20] many rigorous results for the spectrum of the regular NLEP in the complex  $\nu$  plane were obtained. By using the mapping  $\lambda^{(0)\gamma} = \nu$ , these previous results can be used to infer stability or instability for the sub-diffusive case. More specifically, writing  $\nu = |\nu| \exp(i\phi)$  with  $\phi = \arg \nu \in (-\pi, \pi]$ , the map  $\lambda^{(0)\gamma} = \nu$  yields that

$$\lambda^{(0)} = |\nu|^{1/\gamma} e^{i\phi/\gamma}. \quad (43)$$

where  $-\pi < \phi/\gamma \leq \pi$  should hold to remain on the principal branch in the  $\lambda^{(0)}$  plane. The NLEP formulation with sub-diffusion required that  $\Re\lambda^{(0)} \geq 0$  and  $|\lambda^{(0)}| \gg \mathcal{O}(\epsilon)$ . Therefore, in terms of the spectral  $\nu$  plane associated with the regular NLEP, the sub-diffusive system will be unstable if the regular NLEP has an eigenvalue in the following wedge with cutout near the origin, being a subset of the right half-plane  $\Re(\nu) \geq 0$  ( see figure 6 )

$$-\frac{\pi\gamma}{2} \leq \phi \leq \frac{\pi\gamma}{2}, \quad |\nu| \gg \mathcal{O}(\epsilon). \quad (44)$$

The set (44) is the *wedge of instability* of the sub-diffusive NLEP. Notice that the wedge becomes narrower as  $\gamma$  decreases.

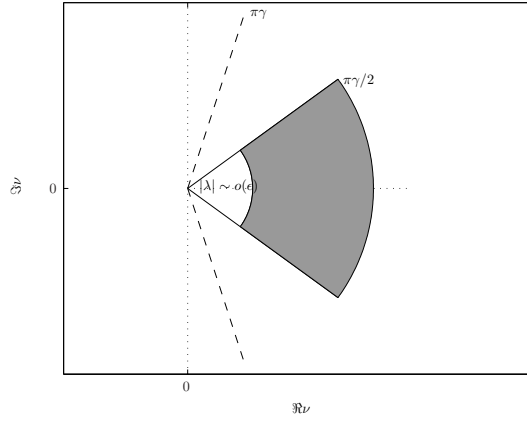


Figure 6: Admissibility and instability region in the  $\nu$  plane ( shaded ) corresponding to the asymptotics validity constraint  $|\lambda| \sim \mathcal{O}(\epsilon)$  or larger. Dashed lines show the region conforming to the principal branch.

A simple consequence of this result is that if the regular NLEP admits a positive real eigenvalue  $\nu^* > 0$ , then this eigenvalue must lie in the wedge of instability for the sub-diffusive NLEP for any  $0 < \gamma < 1$ . Such an eigenvalue  $\lambda^{(0)}$  then yields an exponentially growing perturbation ( to leading order ) to the  $n$ -spike equilibrium solution of the sub-diffusive problem. A sufficient condition for this to occur is the following.

**Theorem 3.1** *Suppose that  $n \geq 2$  and either  $m = 2$  and  $1 < p \leq 5$ , or  $m = p + 1$ . Then, for any  $\tau \geq 0$ , the regular NLEP has a positive real eigenvalue  $\nu^*$  when  $D > D_{th}|_{\gamma=1}$ , where*

$$D_{th}|_{\gamma=1} \stackrel{def}{=} \frac{4}{n^2 \ln^2 \left( \alpha_n + \sqrt{\alpha_n^2 - 1} \right)}, \quad \alpha_n = 1 + \frac{1}{\zeta} \left( 1 + \cos \frac{\pi}{n} \right), \quad \zeta = \frac{qm}{p-1} - s - 1. \quad (45)$$

Consequently, for this range of parameters there is a positive real eigenvalue  $\lambda^{(0)} = (\nu^*)^{1/\gamma}$  that lies in the wedge of instability for the sub-diffusive NLEP.

PROOF Following (5.1) and (5.2) of [20], the eigenvalues for the regular NLEP are the roots of the functions  $g_i(\nu) = 0$  for  $i = 1, \dots, n$ , where

$$g_i(\nu) \equiv C_i(\nu) - f(\nu), \quad f(\nu) \equiv \frac{\int_{-\infty}^{\infty} u^{m-1} (\mathcal{L}_0 - \nu)^{-1} u^p dy}{\int_{-\infty}^{\infty} u^m dy}. \quad (46)$$

Here  $\mathcal{L}_0 = \frac{d^2}{dy^2} - 1 + pu^{p-1}$  is the local operator, and from (38) the functions  $C_i(\nu) \equiv \chi_i^{-1}$  are given by

$$C_i(\nu) = \frac{s}{qm} + \frac{\sqrt{1 + \tau\nu}}{qm \tanh(\theta_o/n)} \left( \tanh \frac{\theta}{n} + \frac{1 - \cos(\pi(i-1)/n)}{\sinh(2\theta/n)} \right). \quad (47)$$

In order to prove that there is a positive real eigenvalue it suffices to consider (46) with  $i = n$ . Proposition 5.1 of [20] proves that  $C_n(0) > 1/(p-1)$  whenever  $D > D_{th}|_{\gamma=1}$ . In addition, Proposition 5.1 of [20] proves that when  $\nu$  is real, then  $C'_n(\nu) \geq 0$  for all  $\nu > 0$  for any  $\tau \geq 0$ . Under the stated conditions on the exponents  $p$  and  $m$ , Proposition 3.5 of [20] proves that  $f(0) = 1/(p-1)$  and that  $f'(\nu) > 0$  on  $0 < \nu < \nu_{loc}$  with  $f(\nu) \rightarrow +\infty$  as  $\nu \rightarrow \nu_{loc}^-$ , where  $\nu_{loc} > 0$  is the unique positive real eigenvalue of the local operator  $\mathcal{L}_0$ . Hence, there must exist a unique root to  $g_n(\nu) = 0$  on  $0 < \nu < \nu_{loc}$ . ■

**Remark 3.3** *Theorem 3.1 gives a sufficient condition for the sub-diffusive system to exhibit instability. Note that when  $D > D_{th}|_{\gamma=1}$  and  $\tau$  is sufficiently large, the regular NLEP can have many unstable eigenvalues, i.e. ones with  $\Re \nu > 0$  (cf. [20]). However, for a fixed value of  $\gamma$ , it is rather difficult to know precisely whether these eigenvalues of the regular NLEP lie within the wedge of instability for the sub-diffusive NLEP.*

The next result for the special case  $\tau = 0$  gives a simple condition to guarantee that there are no eigenvalues  $\nu$  of the regular NLEP problem in the wedge of instability for the sub-diffusive case.

**Theorem 3.2** *Suppose that  $n \geq 2$ ,  $\tau = 0$ , and  $D < D_{th}|_{\gamma=1}$  and that either  $m = 2$  and  $1 < p \leq 5$ , or  $m = p + 1$ . Then, any eigenvalue of the regular NLEP satisfies  $\Re \nu < 0$ . Consequently, there are no eigenvalues in the wedge of instability for the sub-diffusive NLEP.*

PROOF The proof of this result is given in Proposition 5 of [17]. ■

**Remark 3.4** *For the special case  $\tau = 0$  and  $n \geq 2$ , combining Theorems 3.1 and 3.2 allows to conclude that the threshold  $D_{th}|_{\gamma=1}$  still essentially provides the threshold for the sub-diffusive case. However, since the sub-diffusive NLEP formulation required that  $|\lambda^{(0)}| \geq \mathcal{O}(\epsilon)$ , one cannot examine in detail the eigenvalues close to the onset of instability, namely when  $|D - D_{th}|_{\gamma=1}| \ll 1$ .*

In the next two subsections Hopf bifurcations characterised by critical values of  $\tau$  are considered for the case of one and two spike equilibrium solutions.

## 3.2 Hopf bifurcation

### 3.2.1 One-spike equilibrium solution

For the case of a one spike equilibrium solution the threshold  $D_{th}|_{\gamma=1}$  is undefined. When  $D$  is not exponentially large as  $\epsilon \rightarrow 0$ , it is known for the regular NLEP problem that the stability is lost due to a Hopf bifurcation when  $\tau$  exceeds some critical value (cf. [20]).

The eigenvalues of the regular NLEP are the roots  $\nu$  of  $g(\nu) = 0$ , where

$$g(\nu) \equiv C(\nu) - f(\nu), \quad f(\nu) \equiv \frac{\int_{-\infty}^{\infty} u^{m-1} (\mathcal{L}_0 - \nu)^{-1} u^p dy}{\int_{-\infty}^{\infty} u^m dy}. \quad (48)$$

In [20] the following rigorous results on the spectrum of the regular NLEP (48) were obtained.

**Theorem 3.3** *Assume that  $\tau > 0$ ,  $m = 2$ , and  $p > 1$ . Then for any  $D > 0$  the number of eigenvalues  $M$  of (48) in the right half-plane  $\Re \nu > 0$  is either  $M = 0$  or  $M = 2$ .*

**Theorem 3.4** *Suppose that either  $m = 2$  and  $p = 2$ , or  $m = p + 1$  and  $1 < p \leq 5$ . Then, for any  $D > 0$ , there exists a value  $\tau_{0c} = \tau_{0c}(D) > 0$ , such that there are exactly two eigenvalues of (48) on the positive real axis for all  $\tau > \tau_{0c}$ . These two roots are in the interval  $0 < \nu < \nu_{loc}$ . For  $\tau > \tau_{0c}$ , and  $m = 2$ , these are the only two eigenvalues in the right half-plane. In the limit  $\tau \rightarrow \infty$  one of these eigenvalues tends to zero, while the other eigenvalue tends to  $\nu_{loc}$ . This also proves the existence of a value  $\tau_{0H}(D) > 0$  such that there is a pair of complex conjugate eigenvalues on the imaginary axis when  $\tau = \tau_{0H}(D)$ .*

Theorems 3.3 and 3.4 were proved in Propositions 3.4 and 3.7, respectively, of [20]. For the sub-diffusive NLEP problem the proof in [20] of Theorem 3.3 must be modified slightly since the mapping  $\lambda^{(0)\gamma} = \nu$  generates possible points of non-analyticity. This is done in Appendix A, where a result analogous to Theorem 3.3 is proved for the sub-diffusive NLEP. Theorem 3.4, characterising the spectrum on the positive real axis, pertains directly to the sub-diffusive NLEP since  $\lambda^{(0)}$  is real and positive whenever  $\nu$  is real and positive.

The numerical results in [20] for the spectrum of the regular NLEP suggest that results stronger than Theorems 3.3 and 3.4 in fact hold. Namely, for a wide class of exponent sets, the numerical results of [20] indicate that there is a unique value  $\tau_{0H}$  of  $\tau$  for which the regular NLEP (48) has a complex conjugate pair of imaginary eigenvalues  $\nu = \pm i\nu_{0H}$ . Furthermore, for  $\tau > \tau_{0H}$  the paths of unstable complex conjugate

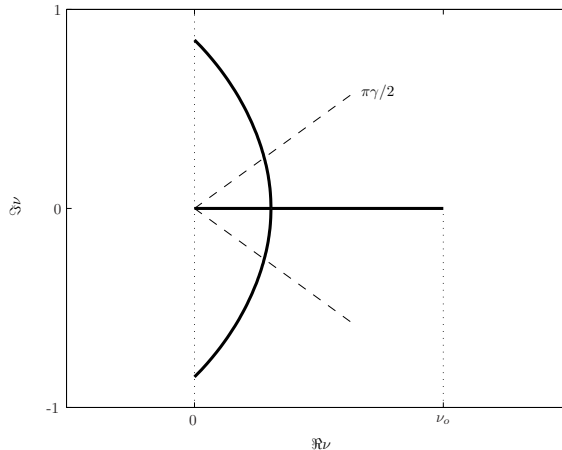


Figure 7: The eigenvalue path, parameterised by  $\tau$ , for the regular NLEP in the complex  $\nu$  plane is plotted, together with the  $\gamma$ -dependent instability wedge for the sub-diffusive NLEP. For  $\tau > \tau_{0H}$  a complex conjugate pair of eigenvalues is in the right half-plane, and they merge onto the real axis at  $\nu = \nu_0 > 0$  when  $\tau = \tau_{0c} > \tau_{0H}$ . For  $\tau > \tau_{0c}$  the eigenvalues remain on the positive real axis with one eigenvalue tending to zero and the other tending to  $\nu_{1oc}$  as  $\tau \rightarrow \infty$ . The system parameters are  $(p, q, m, s) = (2, 1, 2, 0)$  and  $D = 1$ .

eigenvalues in  $\Re\nu > 0$  merge onto the positive real axis at value  $\nu = \nu_0 > 0$  when  $\tau = \tau_{0c}(D) > \tau_{0H}(D)$ . For  $\tau > \tau_{0c}$  one of the real eigenvalues tends to the origin while the other eigenvalue tends to  $\nu_{1oc}$  as  $\tau \rightarrow \infty$ . In figure 7 the numerically computed path of the eigenvalues of the regular NLEP are shown for the case  $D = 1$  and exponent set  $(p, q, m, s) = (2, 1, 2, 0)$ .

The following conjecture is based on the numerical results of [20] and has been validated numerically for various exponent sets  $(p, q, m, s)$ .

**Conjecture 3.1** *There is a unique value  $\tau_{0H}$ , for which the regular NLEP has a Hopf bifurcation. For  $\tau_{0H} < \tau < \tau_{0c}$ , the path  $\nu = \nu(\tau)$  of the complex eigenvalue in the first quadrant is such that  $\Re\nu$  ( $\Im\nu$ ) increases (decreases) monotonically as  $\tau$  increases. When  $\tau = \tau_{0c}$  the regular NLEP has a positive real eigenvalue  $\nu_0$  of multiplicity two.*

The key observation is that an unstable eigenvalue of the regular NLEP only generates an instability for the sub-diffusive NLEP when it lies within the wedge of instability (44). This wedge of instability becomes narrower as the anomaly exponent  $\gamma$  decreases. Therefore under Conjecture 3.1 one concludes that the Hopf bifurcation threshold  $\tau_H$  for the sub-diffusive NLEP increases when the anomaly exponent  $\gamma$  decreases. The anomaly dependent threshold  $\tau_H$  is computed numerically from the implicit condition that

$$\arg \nu = \frac{\pi\gamma}{2}, \quad (49)$$

which involves the eigenvalue path  $\nu = \nu(\tau)$  of the regular NLEP (48) that satisfies  $\Re\nu > 0$ . Condition (49) corresponds to the minimum value of  $\tau$  for which this eigenvalue path enters the wedge of instability of the sub-diffusive NLEP. In this sense, when Conjecture 3.1 holds, it follows that, in comparison with the regular GM model, the sub-diffusive GM model admits a larger range of values of  $\tau$  for which a one spike solution is stable. This leads to the following result.

**Proposition 3.2** *Assume that Conjecture 3.1 for the regular NLEP holds. Then the Hopf bifurcation threshold  $\tau_H$  of the sub-diffusive NLEP increases when the anomaly exponent  $\gamma$  decreases. In particular,  $\tau_H \rightarrow \tau_{0H}$  as  $\gamma \rightarrow 1^-$  and  $\tau_H \rightarrow \tau_{0c}$  as  $\gamma \rightarrow 0^+$ . Therefore, the maximum value of  $\tau$  for which a Hopf bifurcation occurs for the sub-diffusive NLEP is the critical value  $\tau_{0c}$ , and this occurs only in the limit  $\gamma \rightarrow 0^+$ .*

Figure 8 shows numerical results, computed from (44) and (48), for the dependence of the Hopf bifurcation threshold  $\tau_H$  on the anomaly exponent  $\gamma$  for a few values of  $D$ .

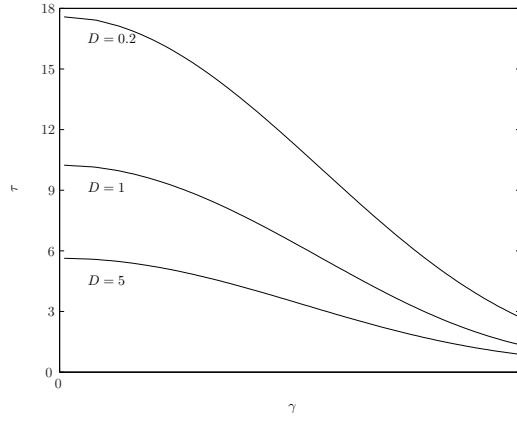


Figure 8: The dependence of the Hopf bifurcation threshold  $\tau_H$  on the anomaly exponent  $\gamma$  for several values of  $D$  corresponding to a one spike equilibrium solution. System parameters used  $(p, q, m, s) = (2, 1, 2, 0)$ .

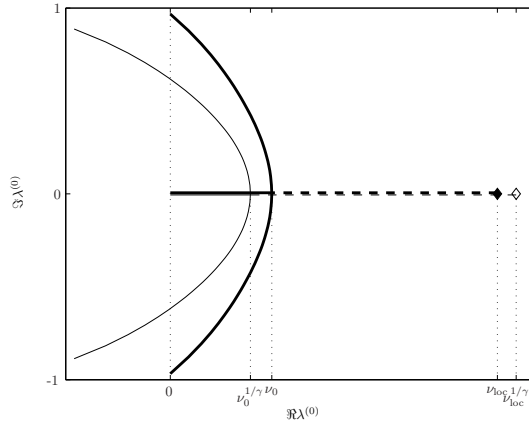


Figure 9: Paths of  $\lambda^{(0)}$  for  $\gamma = 1$  ( thick curve, regular diffusion ) and  $\gamma = 0.8$  ( thin curve, sub-diffusion ). The conjugate pair of eigenvalues corresponds to  $\tau \sim \mathcal{O}(1)$ . As  $\tau$  exceeds a critical value, the complex conjugate eigenvalues become real with one tending to the eigenvalue of the local problem  $\nu_{loc}^{1/\gamma}$  ( dashed line ) and other tending to zero ( solid line ) as  $\tau \rightarrow \infty$ . The system parameters are  $(p, q, m, s) = (2, 1, 2, 0)$  and  $D = 1$  ( then  $\nu_{loc} = 1.25$  ).

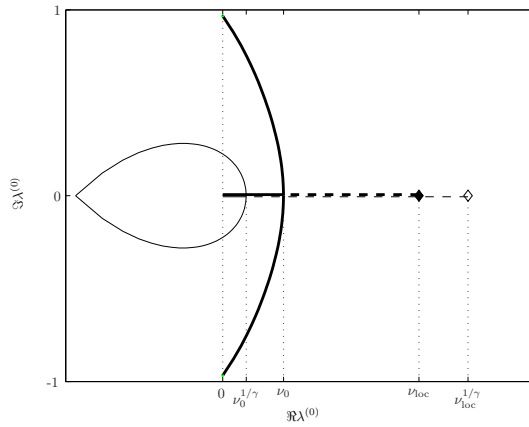


Figure 10: Paths of  $\lambda^{(0)}$  for  $\gamma = 1$  ( thick curve, regular diffusion ) and  $\gamma = 0.5$  ( thin curve, sub-diffusion ). The conjugate pair of eigenvalues corresponds to  $\tau \sim \mathcal{O}(1)$ . As  $\tau$  exceeds a critical value, the complex conjugate eigenvalues become real with one tending to the eigenvalue of the local problem  $\nu_{loc}^{1/\gamma}$  ( dashed line ) and other tending to zero ( solid line ) as  $\tau \rightarrow \infty$ . The system parameters used are  $(p, q, m, s) = (2, 1, 2, 0)$  and  $D = 1$  ( then  $\nu_{loc} = 1.25$  ).

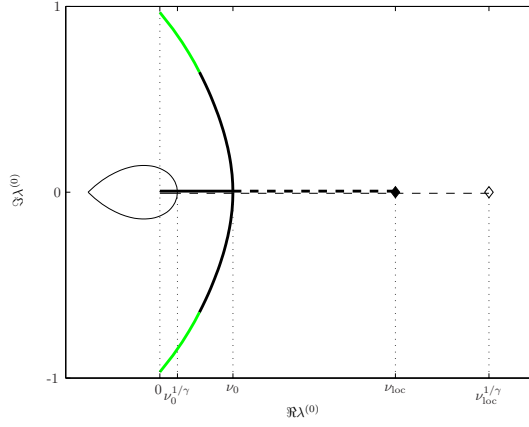


Figure 11: Paths of  $\lambda^{(0)}$  for  $\gamma = 1$  ( thick curve, regular diffusion ) and  $\gamma = 0.4$  ( thin curve, sub-diffusion ). A part of the normal curve satisfying  $|\arg \lambda(0)^\gamma| > \pi\gamma$  was discarded in the computation of the anomalous curve ( shown in grey ). The conjugate pair of eigenvalues corresponds to  $\tau \sim \mathcal{O}(1)$ . As  $\tau$  exceeds a critical value, the complex conjugate eigenvalues become real with one tending to the eigenvalue of the local problem  $\nu_{loc}^{1/\gamma}$  ( dashed line ) and other tending to zero ( solid line ) as  $\tau \rightarrow \infty$ . The system parameters are  $(p, q, m, s) = (2, 1, 2, 0)$  and  $D = 1$  ( then  $\nu_{loc} = 1.25$  ).

Figures 9-11 compare the eigenvalues of the sub-diffusive NLEP with the case  $\gamma = 1$  corresponding to regular diffusion studied in [20]. The comparison is done in the  $\lambda^{(0)}$  plane. Some part of the anomalous eigenvalue curve is located in the left half plane, whereas for the same system parameters with normal diffusion the eigenvalues are unstable. When  $0 < \gamma < \frac{1}{2}$  only a part of the normal curve can be used to compute the eigenvalues of the sub-diffusive NLEP since the principal branch condition  $|\arg \lambda^{(0)\gamma}| < \pi\gamma$  must be satisfied.

### 3.2.2 Asymptotics for $0 < \gamma \ll 1$

When  $\gamma \rightarrow 0$ , the wedge of instability shrinks into the positive real line excluding the origin. Therefore it is possible to derive an asymptotic expression for the shape of the eigenvalues' path providing that the separation of diffusivity scales of the two species is preserved, i.e.  $\epsilon \sim o(\gamma)$  or  $\lim_{\substack{\epsilon \rightarrow 0 \\ \gamma \rightarrow 0}} \epsilon^\gamma = 0$ , so that the spike pattern exists.

Using the mapping  $\lambda^{(0)\gamma} \mapsto \lambda^{(0)}$ , the behaviour of the real eigenvalues  $\lambda_+^{(0)}$  and  $\lambda_-^{(0)}$  at  $\tau \rightarrow \infty$  is determined as follows. First, the larger real eigenvalue  $\lambda_+^{(0)}$  satisfies

$$\lim_{\tau \rightarrow \infty} \lambda_+^{(0)} \Big|_{\gamma < 1} \geq \lim_{\tau \rightarrow \infty} \lambda_+^{(0)} \Big|_{\gamma = 1} \quad \text{if } \nu_{loc} \geq 1.$$

In particular, for  $\nu_{loc} > 1$

$$\lim_{\substack{\tau \rightarrow \infty \\ \gamma \rightarrow 0}} \lambda_+^{(0)} = \lim_{\gamma \rightarrow 0} \nu_{loc}^{1/\gamma} = \infty.$$

On the other hand, for  $\nu_{loc} < 1$

$$\lim_{\substack{\tau \rightarrow \infty \\ \gamma \rightarrow 0}} \lambda_+^{(0)} = \lim_{\gamma \rightarrow 0} \nu_{loc}^{1/\gamma} = 0.$$

In a similar fashion

$$\lim_{\substack{\tau \rightarrow \infty \\ \gamma \rightarrow 0}} \lambda_-^{(0)} = \lim_{\gamma \rightarrow 0} \nu_0^{1/\gamma} = \begin{cases} \infty & \nu_0 > 1 \\ 0 & \nu_0 < 1 \end{cases}.$$

So the two real eigenvalues can chase each other to infinity if  $1 < \nu_0 < \nu_{loc}$  or to the origin if  $0 < \nu_0 < \nu_{loc} < 1$ . The curve is least distorted in the case when  $\lambda_-^{(0)} \rightarrow 0$  and  $\lambda_+^{(0)} \rightarrow \infty$ , i.e. with  $0 < \nu_0 < 1$  and  $\nu_{loc} > 1$ , as happens for the set  $(p, q, m, s) = (2, 1, 2, 0)$ .

The complex conjugate part of the curve shrinks into the origin at the limit  $\gamma \rightarrow 0$  if  $0 < \nu_0 < 1$ , and would expand indefinitely if  $\nu_0 > 1$ . So when  $\nu_0 \leq 1$

$$\left| \frac{d}{d\tau} \lambda^{(0)} \right|_{\gamma < 1} \leq \left| \frac{d}{d\tau} \lambda^{(0)} \right|_{\gamma = 1},$$

as the eigenvalue changes less ( more ) than for the regular curve, and at the limit  $\tau \rightarrow \infty$   $\frac{d}{d\tau} |\lambda^{(0)}|$  will obviously vanish if  $0 < \nu_0 < 1$ , but might not vanish if  $\nu_0 > 1$ . Since at  $0 < \gamma \ll 1$  the complex part of the anomalous curve is generated from the small region about the point  $\nu_0$ , at  $\gamma = 0$  there are no complex eigenvalues. This implies that no Hopf bifurcation is possible. Then if in the corresponding normal system  $0 < \nu_0 < 1$ , there is a triple zero eigenvalue. If in addition  $0 < \nu_{loc} < 1$ , there will be a quadruple zero eigenvalue. If  $1 < \nu_0 < \nu_{loc}$ , there will be a double zero eigenvalue and two infinite eigenvalues.

For  $0 < \gamma \ll 1$  the complex curve near  $\nu_0$  can be approximated by the parabola

$$\Re \lambda^{(0)\gamma} \sim \nu_0 + \frac{1}{2} \alpha \left( \Im \lambda^{(0)\gamma} \right)^2 + \dots, \quad \alpha = \frac{d^2 \Re \lambda^{(0)\gamma}}{d \left( \Im \lambda^{(0)\gamma} \right)^2} < 0 \quad (50)$$

regardless of whether  $\nu_0 \leq 1$ . The parameter  $\alpha$  is related to the curvature of the complex branch when it merges into the real axis and can be uniquely determined for each set  $(p, q, m, s)$ . Using the polar coordinates  $\lambda^{(0)} = \rho e^{i\varphi}$  yields a quadratics for  $\rho^\gamma$

$$\rho^\gamma \cos(\gamma\varphi) \sim \nu_0 + \frac{\alpha}{2} \rho^{2\gamma} \sin^2(\gamma\varphi),$$

which has only one positive solution since  $\alpha < 0$

$$\rho \sim \left( \frac{\cos(\gamma\varphi)}{\alpha \sin^2(\gamma\varphi)} \left\{ 1 - \sqrt{1 - 2\alpha\nu_0 \tan^2(\gamma\varphi)} \right\} \right)^{1/\gamma}.$$

This is a parametrised form of the asymptotics for the complex branch. Since the small portion of the normal curve approximated in this manner generates the whole anomalous complex curve, the asymptotics holds for all  $-\pi < \varphi \leq \pi$ , though the accuracy is not uniform. Figures 12, 13 show the comparison of the full numerical solution and the asymptotics for  $\gamma = 0.2$  and  $\gamma = 0.5$ . Also, the symmetry  $\varphi \leftrightarrow \gamma$  implies that the asymptotics holds for any value of  $\gamma$  for small  $\varphi$ , as expected, however the accuracy deteriorates when either parameter grows, as can be seen from figure 13. Figure 14 shows the maximal error in the parametrised modulus relatively to the true modulus  $|\lambda^{(0)}|$  for the interval of  $\gamma$ , where the anomalous complex curve can be obtained from the normal curve for  $-\pi < \varphi \leq \pi$ , i.e.  $0 < \gamma < \frac{1}{2}$ . Note that  $\alpha$  was estimated only once regardless of the value of  $\gamma$ .

The asymptotics shows how the magnitude of the eigenvalues at the limit  $\gamma \rightarrow 0$  depends on  $\nu_0$ . Using the identities

$$\lim_{x \rightarrow 0} (1+x)^{1/x} = e \quad \rightarrow \quad \lim_{x \rightarrow 0} (1 + \tilde{k}x)^{1/x} = \lim_{\zeta \rightarrow 0^{\text{sgn } \tilde{k}}} (1 + \zeta)^{\tilde{k}/\zeta} = e^{\tilde{k}},$$

it is obtained that

$$\lim_{\gamma \rightarrow 0} \rho = \lim_{\gamma \rightarrow 0} \nu_0^{1/\gamma} \left\{ 1 + \left( \frac{1}{3} + \frac{1}{2} \alpha \nu_0 \right) \gamma^2 \varphi^2 + \mathcal{O}(\gamma^4) \right\}^{1/\gamma} < \lim_{\gamma \rightarrow 0} \nu_0^{1/\gamma} e^{\varphi \sqrt{|k|}}, \quad k = \frac{1}{3} + \frac{1}{2} \alpha \nu_0 + \mathcal{O}(\gamma^2)$$

or

$$\lim_{\gamma \rightarrow 0} \rho = \begin{cases} 0 & 0 < \nu_0 < 1 \\ \exp(\varphi \sqrt{|k|}) & \nu_0 = 1 \\ \infty & \nu_0 > 1. \end{cases}$$

Thus but for the special value  $\nu_0 = 1$ , the magnitude of the eigenvalues is determined by the value of  $\nu_0$ , yielding either a shrinking to the origin or expanding indefinitely closed curve.

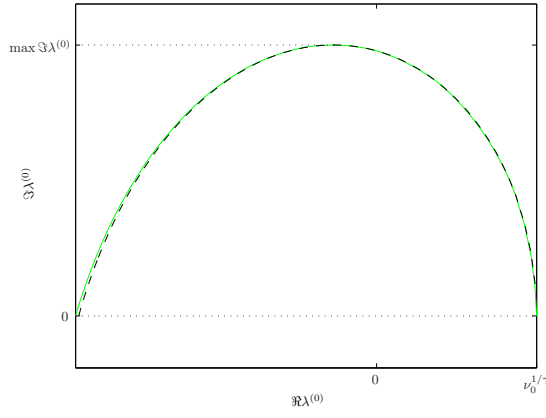


Figure 12: Complex branch of  $\lambda^{(0)}$  for  $\gamma = 0.2$  ( showing only  $\Im\lambda^{(0)} \geq 0$  ): full numerical solution ( green, solid ) and asymptotics by parabolic approximation of  $\lambda^{(0)\gamma}$  in the vicinity of  $\nu_0$ . System parameters used  $(p, q, m, s) = (2, 1, 2, 0)$  and  $D = 1$  ( then  $\nu_{loc} = 1.25$  ).

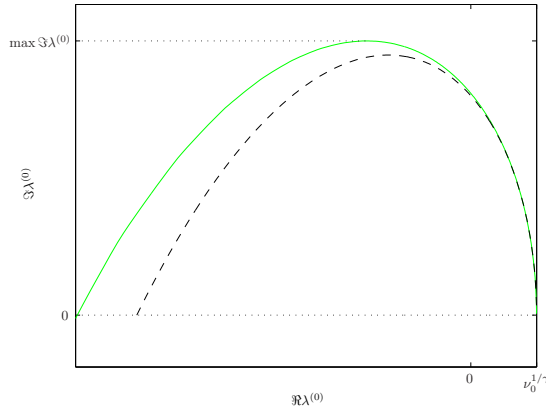


Figure 13: Complex branch of  $\lambda^{(0)}$  for  $\gamma = 0.5$  ( showing only  $\Im\lambda^{(0)} \geq 0$  ): full numerical solution ( green, solid ) and asymptotics by parabolic approximation of  $\lambda^{(0)\gamma}$  in the vicinity of  $\nu_0$ . System parameters used  $(p, q, m, s) = (2, 1, 2, 0)$  and  $D = 1$  ( then  $\nu_{loc} = 1.25$  ).

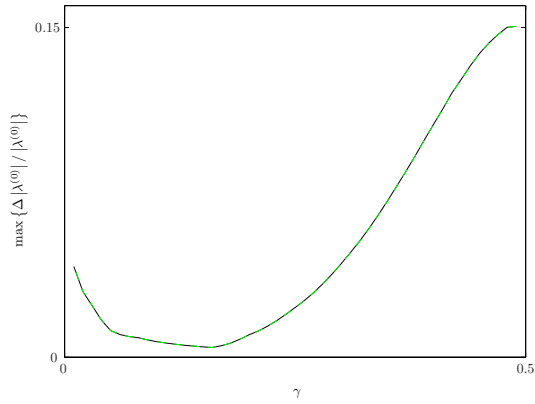


Figure 14: Maximal error of the asymptotics of the parametrised modulus  $\rho(\varphi)$  normalised by  $|\lambda^{(0)}|$  for  $0 < \gamma < \frac{1}{2}$ .

The asymptotics for  $\alpha$  is derived as follows. Equation (48) in its explicit form

$$\frac{1}{\chi} = \frac{1}{qm} \left( s + \frac{\theta \tanh \theta}{\theta_o \tanh \theta_o} \right) = \frac{1}{b_m} \int_{-\infty}^{\infty} u^{m-1} \left( \mathcal{L}_0 - \lambda^{(0)} \right)^{-1} u^p dy,$$

can be differentiated with respect to  $\tau$  since it is in fact an equation for the function  $\lambda^{(0)}(\tau)$ :

$$\frac{\tanh \theta / \theta + \operatorname{sech}^2 \theta}{2Dqm\theta_o \tanh \theta_o} \left\{ \lambda^{(0)} + \tau \frac{d\lambda^{(0)}}{d\tau} \right\} = \frac{1}{b_m} \int_{-\infty}^{\infty} u^{m-1} \left( L_0 - \lambda^{(0)} \right)^{-2} u^p dy \frac{d\lambda^{(0)}}{d\tau}. \quad (51)$$

Define  $\bar{\lambda}^{(0)} = \lambda_r + i\lambda_i$ ,  $\lambda_r, \lambda_i \in \mathbb{R}$ , use  $\theta(\tau) = \theta_o \sqrt{1 + \tau \lambda^{(0)}}$  to evaluate (51) at  $\tau = \tau_{0c}^-$ , so that  $\lambda_r = \nu_0$ ,  $\lambda_i = 0$ ,  $\theta_c = \theta(\tau_{0c})$  and extract imaginary and real parts to get

$$(I - \tau_{0c}K) \frac{d\lambda_i}{d\tau} \Big|_{\tau_{0c}^-} = 0, \quad (I - \tau_{0c}K) \frac{d\lambda_r}{d\tau} \Big|_{\tau_{0c}^-} = K\nu_0,$$

$$K = \frac{\tanh \theta_c / \theta_c + \operatorname{sech}^2 \theta_c}{2Dqm\theta_o \tanh \theta_o}, \quad I = \frac{1}{b_m} \int_{-\infty}^{\infty} u^{m-1} (L_0 - \nu_0)^{-2} u^p dy.$$

Since  $\frac{d\lambda_i}{d\tau} \Big|_{\tau_{0c}^-} \neq 0$ ,  $I - \tau_{0c}K = 0$  must hold. Then the second equation can only be satisfied if  $\frac{d\lambda_r}{d\tau} \Big|_{\tau_{0c}^-} = \infty$ .

Now divide (51) by  $\frac{d\lambda_i}{d\tau} \Big|_{\tau_{0c}^-}$  to have

$$K \left\{ \nu_0 / \frac{d\lambda_i}{d\tau} \Big|_{\tau_{0c}^-} + \tau_{0c} \left( \frac{d\lambda_r}{d\lambda_i} \Big|_{\tau_{0c}^-} + i \right) \right\} = I \left( \frac{d\lambda_r}{d\lambda_i} \Big|_{\tau_{0c}^-} + i \right).$$

Bearing in mind that

$$\frac{d\lambda_r}{d\lambda_i} \Big|_{\tau_{0c}^-} = \frac{d\lambda_r}{d\tau} \Big|_{\tau_{0c}^-} / \frac{d\lambda_i}{d\tau} \Big|_{\tau_{0c}^-} = 0 \quad (52)$$

gives  $\frac{d\lambda_i}{d\tau} \Big|_{\tau_{0c}^-} = \infty$  ( otherwise the real part remains unmatched ) and

$$\frac{d\lambda_r}{d\tau} \Big|_{\tau_{0c}^-} \sim o \left( \frac{d\lambda_i}{d\tau} \Big|_{\tau_{0c}^-} \right).$$

Since both derivatives  $\frac{d\lambda_r}{d\tau} \Big|_{\tau_{0c}^-}$ ,  $\frac{d\lambda_i}{d\tau} \Big|_{\tau_{0c}^-}$  are infinite, no Taylor series for  $\lambda_r(\tau)$  and  $\lambda_i(\tau)$  in the neighbourhood of  $\tau_{0c}^-$  exist. As the values are finite  $\lambda_r(\tau_c) = \nu_0$ ,  $\lambda_i(\tau_c) = 0$ , fractional powers can give the asymptotics

$$\lambda_r \sim \nu_0 + c_r (\tau_c - \tau_0)^{\beta_r}, \quad c_r < 0, \quad 0 < \beta_r < 1,$$

$$\lambda_i \sim c_i (\tau_c - \tau_0)^{\beta_i}, \quad c_i \geq 0, \quad 0 < \beta_i < 1,$$

with  $\beta_r > \beta_i$  for (52) to hold. Using these in

$$\alpha = \frac{d^2 \lambda_r}{d\lambda_i^2} = \frac{d}{d\tau_0} \left( \frac{d\lambda_r}{d\tau_0} \Big|_{\tau_c^-} / \frac{d\lambda_i}{d\tau_0} \Big|_{\tau_c^-} \right) \frac{d\tau_0}{d\lambda_i} = \frac{d^2 \lambda_r}{d\tau_0^2} / \left( \frac{d\lambda_i}{d\tau_0} \right)^2 - \frac{d\lambda_r}{d\tau_0} \frac{d^2 \lambda_i}{d\tau_0^2} / \left( \frac{d\lambda_i}{d\tau_0} \right)^3$$

and recalling that  $\alpha$  should be a constant,  $\beta_r = 2\beta_i < 1$ , also giving  $\beta_i < \frac{1}{2}$  and  $\alpha = \frac{2c_r}{c_i^2} < 0$ .

### 3.2.3 Multi-spike equilibrium solution

When  $D < D_{\text{th}}|_{\gamma=1}$ , it is possible to characterise oscillatory instabilities for the case of a multi-spike equilibrium pattern with  $n \geq 2$ . For the regular GM model, it is known from [20] that the  $n$  different regular NLEP's in (38) each have a Hopf bifurcation threshold, labelled by  $\tau = \tau_{0Hi}$ , for  $i = 1, \dots, n$ . The overall Hopf bifurcation threshold  $\tau_{0H}$  is the minimum of these  $n$  individual thresholds. For a wide range of exponent sets the numerical results of [20] for the regular NLEP showed that the threshold  $\tau_{0H}$  is determined by the mode  $i = 1$ , corresponding to a synchronous oscillatory instability in the spike amplitudes.

In contrast, for a sub-diffusive medium with an anomaly exponent  $\gamma$  below a certain threshold, the following result gives a sufficient condition for the asynchronous  $i = n$  mode in (38) to set the Hopf bifurcation threshold for the sub-diffusive NLEP.

**Proposition 3.3** *Suppose that  $n \geq 2$  and  $D < D_{\text{th}}|_{\gamma=1}$ , where  $D_{\text{th}}|_{\gamma=1}$  is defined in (45). Suppose also that either  $m = p + 1$  and  $1 < p \leq 5$ , or  $m = p = 2$ . Then at the limit  $\gamma \rightarrow 0$  the Hopf bifurcation threshold  $\tau_H$  for the sub-diffusive NLEP is determined by the  $i = n$  mode in (38). Moreover,  $\tau_H \rightarrow \tau_{0cn}$ , where  $\tau_{0cn}$  is the value of  $\tau$  for which the regular NLEP (38) with  $i = n$  has a real positive eigenvalue of multiplicity two.*

**PROOF** Consider the regular NLEP (38) with  $D < D_{\text{th}}|_{\gamma=1}$  and a fixed value of  $j$  in  $1 \leq i \leq n$ . Then, the eigenvalues of the regular NLEP are the roots of the functions  $g_i(\nu) \equiv C_i(\nu) - f(\nu) = 0$ , where  $C_i(\nu)$  and  $f(\nu)$  are defined in (46) and (47). Then, there is a threshold  $\tau_{0ci}$  of  $\tau$  for which  $g_i(\nu) = 0$  has a root  $\nu_{0i}$  of multiplicity two (see [20]). Since the wedge of instability (44) collapses onto the positive real axis in the  $\nu$ -plane as  $\gamma$  decreases, it follows that the Hopf bifurcation threshold  $\tau_{Hi}$  for the sub-diffusive NLEP with mode  $i$  satisfies  $\tau_{Hi} \rightarrow \tau_{0ci}$  as  $\gamma \rightarrow 0$ . Since  $\tau_H = \min_{1 \leq i \leq n} \tau_{Hi}$ , the proof is complete if one can prove that the ordering relation  $\tau_{0cn} < \tau_{0ci}$  for  $1 \leq i < n$  for the regular NLEP holds.

To prove this, recall from Proposition 5.1 of [20] that for any  $\nu > 0$  real and any fixed  $\tau > 0$

$$C_n(\nu) > C_{n-1}(\nu) > \dots > C_1(\nu) > 0, \quad 0 < C'_n(\nu) < C'_{n-1}(\nu) < \dots < C'_1(\nu), \quad (53)$$

$$C''_i(\nu) < 0, \quad C'_i(\nu) = \mathcal{O}(\tau^{1/2}), \quad \text{as } \tau \rightarrow +\infty, \quad i = 1, \dots, n. \quad (54)$$

Since  $C_i$  depends on  $\tau$  and  $\nu$  only through the product  $\tau\nu$ , the monotonicity and concavity results for  $C_i$  also hold with respect to  $\tau$ . Furthermore, when either  $m = p + 1$  and  $1 < p \leq 5$ , or  $m = p = 2$ , it was proved in Proposition 3.5 of [20] that for any real  $\nu > 0$

$$f(0) = \frac{1}{p-1}, \quad f'(\nu) > 0, \quad f''(\nu) > 0, \quad \text{on } 0 < \nu < \nu_{\text{loc}},$$

and that  $f(\nu) \rightarrow +\infty$  as  $\nu \rightarrow \nu_{\text{loc}}^-$ .

Therefore, for each  $i$  there is a real positive eigenvalue of multiplicity two for the regular NLEP on the interval  $0 < \nu < \nu_{\text{loc}}$  when  $\tau = \tau_{0ci}$ , characterised by the tangential intersection of the two curves  $C_i(\nu)$  and  $f(\nu)$ . Such a critical value of  $\tau$  must exist since owing to the convexity of  $f$ , the concavity of  $C_i$ , and the fact that  $C_i$  is unbounded as  $\tau \rightarrow \infty$  for any  $\nu > 0$ . Let  $\tau_{0cn}$  denote the value of  $\tau$  for which  $C_n$  and  $f$  intersect tangentially at some value  $\nu = \nu_{0n}$  in  $0 < \nu < \nu_{\text{loc}}$ . Then, by the convexity of  $f$  and concavity of  $C_n$ , it follows that  $g_n(\nu) < 0$  when  $\tau = \tau_{0cn}$  for  $\nu \neq \nu_{0n}$  on  $0 < \nu < \nu_{\text{loc}}$ . Since  $C_i(\nu) < C_n(\nu)$  for  $i \neq n$  from (53), it follows for  $\tau = \tau_{0cn}$  that  $g_i(\nu) < 0$  for  $0 < \nu < \nu_{\text{loc}}$  and any  $i = 1, \dots, n-1$ . Therefore, the smallest value of  $\tau$  for which  $C_i$  and  $f$  intersect tangentially must occur for the mode  $i = n$ . This completes the proof. ■

In figure 15(a) this result is illustrated numerically for two spikes with  $D = 0.5 < D_{\text{th}}|_{\gamma=1}$  by plotting  $f(\nu)$  together with  $C_i(\nu)$  for  $i = 1, 2$  at the value  $\tau = \tau_{0c2} \approx 4.51$ , for which  $C_2(\nu)$  intersects  $f(\nu)$  tangentially. In figure 15(b) the numerically computed path  $\nu = \nu(\tau)$  is shown in the complex plane for the unstable eigenvalue of the regular NLEP for both  $i = 1$  ( synchronous ) and  $i = 2$  ( asynchronous ) modes. The

computations show that  $\Im\nu > 0$  and  $\Re\nu > 0$  when  $1.04 \approx \tau_{0H1} < \tau < \tau_{0c1} \approx 7.13$  for the synchronous mode, and  $2.33 \approx \tau_{0H1} < \tau < \tau_{0c1} \approx 4.51$  for the asynchronous mode. Thus, for  $D = 0.5$ , it is concluded that  $\tau_H \rightarrow 4.51$  when the anomaly exponent  $\gamma \rightarrow 0$ .

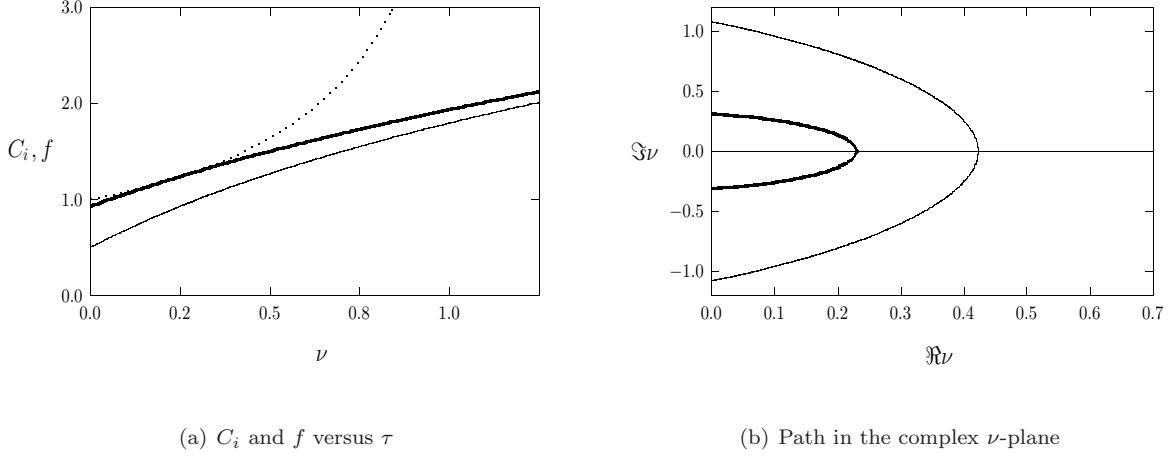


Figure 15: Left: plot of  $C_1(\nu)$  ( solid curve, synchronous instability ),  $C_2(\nu)$  ( heavy solid curve, asynchronous instability ), and  $f(\nu)$  for a two-spike solution with  $D = 0.5$ , and  $\tau = \tau_{0c2} = 4.51$ . At this value of  $\tau$ ,  $C_2$  intersects  $f$  tangentially. Right: plot of the path in the spectrum  $\Im\nu$  versus  $\Re\nu$  for  $D = 0.5$  parameterised by  $\tau$  for the synchronous ( solid curve ) and asynchronous ( heavy solid curve ) modes. The exponent set used  $(p, q, m, s) = (2, 1, 2, 0)$ .

For a two-spike equilibrium solution and two fixed values of  $D$ , the numerically computed synchronous and asynchronous Hopf bifurcation thresholds  $\tau_{Hj}$  for  $i = 1, 2$  versus  $\gamma$  are plotted in figure 16. For  $\gamma$  sufficiently close to  $\gamma = 1$  the synchronous mode sets the threshold, so that  $\tau_H = \tau_{H1}$ , whereas when  $\gamma$  is sufficiently small the asynchronous mode sets the instability threshold. For  $D = 0.5$  the cross-over point is at  $\gamma \approx 0.65$ . For a smaller value of  $D$  the cross-over point occurs for a smaller value of  $\gamma$ .

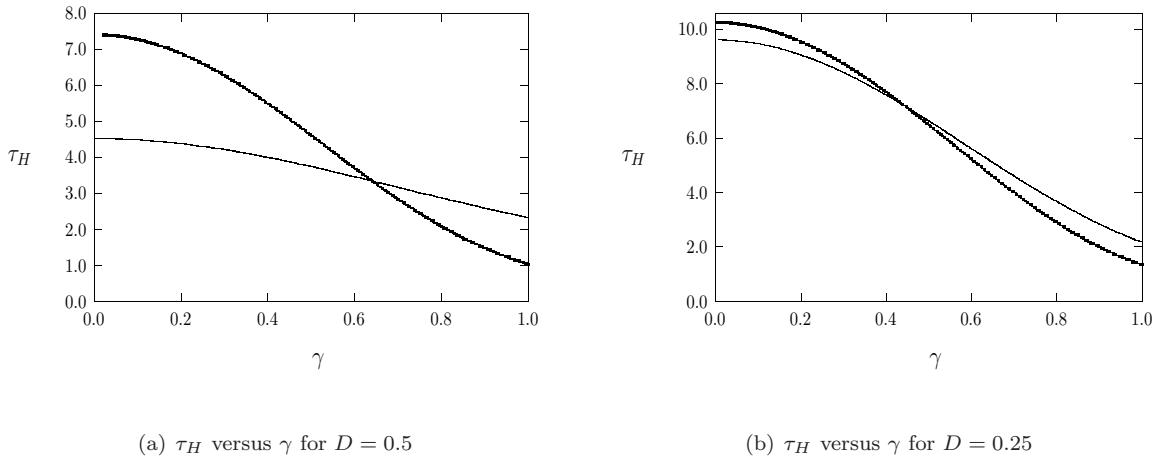


Figure 16: Plot of  $\tau_H$  versus the anomaly exponent  $\gamma$  for  $D = 0.5$  ( left ) and for  $D = 0.25$  ( right ). The exponent set used  $(p, q, m, s) = (2, 1, 2, 0)$ . In each subfigure the threshold for the synchronous instability is the heavy solid curve while the asynchronous instability is the solid curve. The Hopf bifurcation value  $\tau_H$  is the minimum of these two thresholds. For a sufficiently anomalous system (i.e.  $\gamma$  small enough), the asynchronous instability determines  $\tau_H$ .

Finally, figure 17 compares the numerically computed Hopf bifurcation thresholds for synchronous and asynchronous instabilities as function of  $D$  on  $D < D_{th}|_{\gamma=1}$  for a fixed anomaly exponent  $\gamma = 0.5$ . The Hopf bifurcation threshold for the regular diffusion case is also plotted. These results show that even at  $\gamma = 0.5$

the asynchronous instability is the dominant instability for  $D$  sufficiently close to  $D_{\text{th}}|_{\gamma=1}$ .

In conclusion, the results in this sub-section show that sub-diffusion has two main effects on the stability of a multi-spike solution. Firstly, with sub-diffusion there is a larger range of  $\tau$  for which a stable  $n$ -spike equilibrium solution exists when  $D < D_{\text{th}}|_{\gamma=1}$ . Secondly, when  $\gamma$  is sufficiently small, the temporal oscillatory instability is no longer a synchronous oscillatory instability as in the case of regular diffusion. Although we have only numerically studied in detail the case of a two-spike equilibrium solution, similar results can be obtained for equilibrium solutions with  $n > 2$ , and for quasi-equilibrium two-spike solutions (similar to that studied for the case of regular diffusion in [24]). We do not pursue these details here.

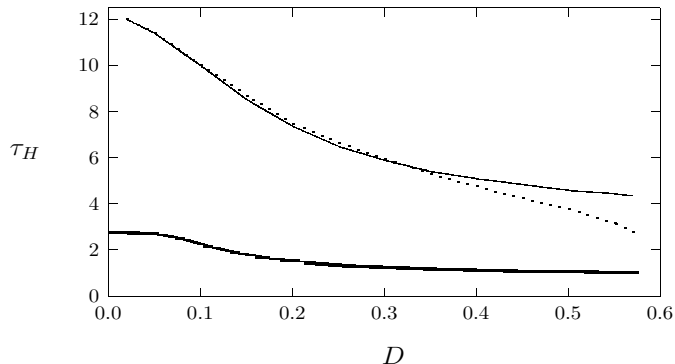


Figure 17: Plot of  $\tau_H$  versus  $D$  on the range  $D < D_{\text{th}}|_{\gamma=1} \approx 0.5766$  for a two-spike equilibrium solution and the exponent set  $(p, q, m, s) = (2, 1, 2, 0)$ . The anomaly exponent for sub-diffusion is  $\gamma = 1/2$ . The solid (dotted) curve corresponds to the synchronous (asynchronous) instability.  $\tau_H$  is the minimum of these two curves. The asynchronous instability dominates for  $D$  close to  $D_{\text{th}}|_{\gamma=1}$ . The heavy solid curve is the Hopf bifurcation threshold for regular diffusion  $\gamma = 1$ .

## 4 Discussion

The DAE system governing the evolution of an  $n$  spike quasi-equilibrium solution to one dimensional GM model was derived for a sub-diffusive medium. The presence of sub-diffusion scales the width of each spike in the pattern according to the anomaly index  $\gamma$ . It was shown that the spike motion in a sub-diffusive medium is asymptotically slower than for the case of regular diffusion studied in [18]. Moreover, the spike centres approach their equilibrium locations algebraically in time, as opposed to the exponential rate in time characteristic of regular diffusion. The DAE system for spike motion with sub-diffusion also differs from the regular one by an anomaly dependent factor  $f(p; \gamma)$  that can be computed numerically for given values of  $p$  and  $\gamma$ . In addition, in a sub-diffusive medium the ratio of diffusivities for the existence of a spike-type solution is  $\mathcal{O}(\epsilon^{-2\gamma})$  with  $0 < \gamma < 1$ , which is asymptotically smaller than the ratio  $\mathcal{O}(\epsilon^{-2})$  required for the case of regular diffusion. The decrease in the required ratio of diffusivities for the existence of spike solutions with sub-diffusion is potentially significant since it is difficult to justify extreme diffusivity ratios when modelling actual biological systems.

The DAE system for spike motion for the sub-diffusive GM model shows that the motion of the spikes centres is governed by separate equations for leftward and rightward motion, in contrast to the case of regular diffusion, where a unique equation governs the motion in both directions. The distinction stems from the intrinsic property of the fractional derivative operator, which in its basic form models memory, i.e. takes into account events that occurred in the past. Due to the inapplicability of many basic calculus tools to fractional derivatives and in particular the chain differentiation rule, using the memory operator as a spatial operator requires a certain care. The leftward motion conforms to a direct use of the fractional derivative, since

the spike moves into a region, whose properties are “in the past” and thus known, whereas the rightward motion results in a slightly modified operator since the spike moves into a region, whose properties are “in the future”.

A stability theory was formulated for disturbances with exponential time behaviour, addressing only the eigenvalues with a positive real part. This limitation is due to the fact that the fractional derivative of order  $0 < \gamma < 1$  of a decaying exponential function  $\frac{d^\gamma}{dt^\gamma} \exp(\lambda^{(0)}t)$ ,  $\Re\lambda^{(0)} < 0$  decays algebraically at  $t \rightarrow \infty$ , as opposed to the exponential decay for the case  $\gamma = 1$ . Thus, within this framework, an eigenvalue can be traced provided that  $\Re\lambda^{(0)} \geq 0$ . When  $\Re\lambda^{(0)} < 0$ , it is known that the eigenvalue is in the left half plane since  $\Re\lambda^{(0)} \neq 0$ , but it cannot be traced. Therefore, only the eigenvalues with a positive real part can be considered correct growth rates for the linearised system at hand.

By using the method of matched asymptotic expansions an NLEP was derived to characterise disturbances with exponential time behaviour. The sub-diffusive NLEP problem with eigenvalue parameter  $\lambda^{(0)}$  is related to the regular NLEP problem with eigenvalue parameter  $\nu$  through the mapping  $\lambda^{(0)\gamma} = \nu$ . The consequence of this is that an unstable eigenvalue  $\nu$  in the right half-plane for the regular NLEP can only generate instability for the sub-diffusive NLEP, when it lies in the wedge of instability defined by  $-\pi\gamma/2 < \arg \nu < \pi\gamma/2$ . Several key observations follow from this result. First, a real positive eigenvalue of the regular NLEP generates instability for the sub-diffusive NLEP. Thus in terms of the diffusivity  $D$  multi-spike equilibrium solutions for the sub-diffusive GM model and the regular GM model have essentially the same stability threshold  $D_{\text{th}}|_{\gamma=1}$  when  $\tau = 0$ , where  $D_{\text{th}}|_{\gamma=1}$  is defined in (45). Secondly, it is shown that the stability of a one-spike equilibrium solution is lost due to a Hopf bifurcation at some  $\tau = \tau_H$ . The threshold  $\tau_H$  is shown to be a decreasing function of the anomaly exponent  $\gamma$ . Thus, introduction of sub-diffusion into the regular GM model yields a larger range in  $\tau$ , where a stable one spike solution can occur. Finally, a novel consequence of the stability theory is that for a multi-spike equilibrium solution with  $D < D_{\text{th}}|_{\gamma=1}$  and  $\tau = \tau_H$ , an asynchronous oscillatory instability of the spike amplitudes dominates when the medium is sufficiently sub-diffusive, i.e. when  $\gamma$  is sufficiently small. This behaviour is in marked contrast to that of the case of regular diffusion, where as shown in [20], the Hopf bifurcation in  $\tau$  corresponds to a synchronous oscillatory instability of the spike amplitudes.

There are a few directions for further enquiry. It would be interesting to develop a numerical method to perform full numerical simulations of spike dynamics for the sub-diffusive GM model, and to test the stability results reported in this paper. Owing to the nonlocality of the memory operator in (2), this would be a highly nontrivial undertaking. Secondly, it would be interesting to extend the present analytical theory to the case of a multi-spatial dimensional domain.

## References

- [1] G. Georgiou, S. S. Bahra, A. R. Mackie, C. A. Wolfe, P. O’Shea, S. Ladha, N. Fernandez, R. J. Cherry, *Measurement of the lateral diffusion of human MHC Class I molecules on HeLa cells by fluorescence recovery after photobleaching using a phycoerythrin probe*, Biophys. J., **82**(4), (2002), pp. 1828–1834.
- [2] A. Masuda, K. Ushida, T. Okamoto, *New fluorescence correlation spectroscopy (FCS) suitable for the observation of anomalous diffusion in polymer solution: Time and space dependencies of diffusion coefficients*, J. Photochem. Photobio. A: Chem., **183**(3), (2006), pp. 304–308.
- [3] K. Dworecki, K. D. Lewandowska, T. Kosztolowicz, *Application of two-membrane system to measure subdiffusion coefficients*, Acta Physica Polonica B, **39**(5), (2008), pp. 1221–1227.
- [4] R. Metzler, J. Klafter, *The random walk’s guide to anomalous diffusion: a fractional dynamics approach*, Phys. Rep., **339**, (2000), pp. 1–77.
- [5] K. B. Oldham, J. Spanier, *The fractional calculus*, Academic Press, New York, 1974.
- [6] I. Podlubny, *Fractional differential equations*, Academic Press, San Diego, 1999.

- [7] R. K. Saxena, A. M. Mathai, H. J. Haubold, *Fractional reaction-diffusion equations*, *Astrophys. Space Sci.*, **305**(3), (2006), pp. 289–296.
- [8] H. Hinrichsen, *Non-equilibrium phase transitions with long-range interactions*, *J. Stat. Mech.: Theor. Exper.*, (2007), P07006.
- [9] Y. Nec, V. A. Volpert, A. A. Nepomnyashchy, *Front propagation problems with sub-diffusion*, *Discr. Cont. Dyn. Sys. Series A*, **27**(2), (2010), pp. 827–846.
- [10] B. I. Henry, S. L. Wearne, *Existence of Turing instabilities in a two-species fractional reaction-diffusion system*, *SIAM J. Appl. Math.*, **62**(3), (2002), pp. 870–887.
- [11] Y. Nec, A. A. Nepomnyashchy, *Linear stability of fractional reaction-diffusion systems*, *Math. Model. Nat. Phenom.*, **2**(2), (2007), pp. 77–105.
- [12] Y. Nec, A. A. Nepomnyashchy, *Turing instability in sub-diffusive reaction-diffusion systems*, *J. Physics A: Math. Theor.*, **40**(49), (2007), pp. 14687–14702.
- [13] A. Doelman, R. A. Gardner, T. J. Kaper, *Stability analysis of singular patterns in the 1D Gray-Scott model: a matched asymptotics approach*, *Physica D*, **122**(1-4), (1998), pp. 1–36.
- [14] J. Wei, *On single interior spike solutions for the Gierer-Meinhardt system: uniqueness and stability estimates*, *Europ. J. Appl. Math.*, **10**(4), (1999), pp. 353–378.
- [15] A. Doelman, W. Eckhaus, T. J. Kaper, *Slowly modulated two-pulse solutions in the Gray-Scott Model I: asymptotic construction and stability*, *SIAM J. Appl. Math.*, **61**(3), (2000), pp. 1080–1102.
- [16] A. Doelman, W. Eckhaus, T. J. Kaper, *Slowly modulated two-pulse solutions in the Gray-Scott model II: geometric theory, bifurcations, and splitting dynamics*, *SIAM J. Appl. Math.*, **61**(6), (2000), pp. 2036–2061.
- [17] D. Iron, M. J. Ward, J. Wei, *The stability of spike solutions to the one-dimensional Gierer-Meinhardt model*, *Physica D*, **150**(1-2), (2001), pp. 25–62.
- [18] D. Iron, M. J. Ward, *The dynamics of multi-spike solutions to the one-dimensional Gierer-Meinhardt model*, *SIAM J. Appl. Math.*, **62**(6), (2002), pp. 1924–1951.
- [19] C. Muratov, V. V. Osipov, *Stability of the static spike autosolitons in the Gray-Scott model*, *SIAM J. Appl. Math.*, **62**(5), (2002), pp. 1463–1487.
- [20] M. J. Ward, J. Wei, *Hopf bifurcations and oscillatory instabilities of spike solutions for the one-dimensional Gierer-Meinhardt model*, *J. Nonl. Sci.*, **13**(2), (2003), pp. 209–264.
- [21] H. van der Ploeg, A. Doelman, *Stability of spatially periodic pulse patterns in a class of singularly perturbed reaction-diffusion equations*, *Indiana U. Math. J.*, **54**(5), (2005), pp. 1219–1301.
- [22] T. Kolokolnikov, M. Ward, J. Wei, *The stability of spike equilibria in the one-dimensional Gray-Scott model: the low feed-rate regime*, *Studies in Appl. Math.*, **115**(1), (2005), pp. 21–71.
- [23] T. Kolokolnikov, M. Ward, J. Wei, *The stability of spike equilibria in the one-dimensional Gray-Scott model: the pulse-splitting regime*, *Physica D*, **202**(3-4), (2005), pp. 258–293.
- [24] W. Sun, M. J. Ward, R. Russell, *The slow dynamics of two-spike solutions for the Gray-Scott and Gierer-Meinhardt systems: competition and oscillatory instabilities*, *SIAM J. App. Dyn. Systems*, **4**(4), (2005), pp. 904–953.
- [25] A. Doelman, T. Kaper, K. Promislow, *Nonlinear asymptotic stability of the semi-strong pulse dynamics in a regularized Gierer-Meinhardt model*, *SIAM J. Math. Anal.*, **38**(6), (2007), pp. 1760–1789.
- [26] W. Chen, M. J. Ward, *Oscillatory instabilities of multi-spike patterns for the one-dimensional Gray-Scott model*, *Europ. J. Appl. Math.*, **20**(2), (2009), pp. 187–214.

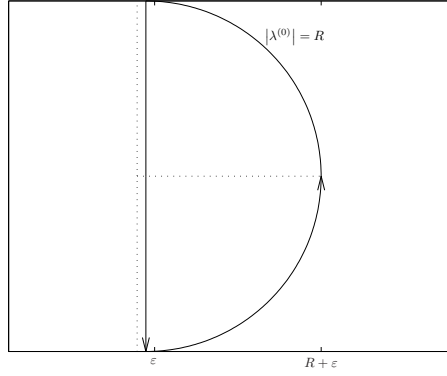


Figure 18: Closed contour in the calculation of number of eigenvalues in the right half plane.

## A Calculation of the winding number for a one-spike solution

In this appendix a result analogous to Theorem 3.3 is proved for the sub-diffusive NLEP problem.

**Proposition A.1** Define  $\tilde{C}(\lambda^{(0)}) = C(\lambda^{(0)\gamma})$ , where  $C(\nu)$  is defined in (48). Then,  $\tilde{C}(\lambda^{(0)})$  has a single non-analytic point  $\lambda^{(0)} = 0$  on the principal branch  $-\pi < \arg \lambda^{(0)} \leq \pi$ .

PROOF By direct differentiation

$$\tilde{C}'(\lambda^{(0)}) = \frac{\tau\theta_o}{2qm \tanh \theta_o} \left( \frac{\tanh \theta}{\theta} + \operatorname{sech}^2 \theta \right) \gamma \lambda^{(0)\gamma-1},$$

which yields the four possible singular points

$$\lambda_1^{(0)} = 0, \quad \lambda_2^{(0)} = \left(\frac{1}{\tau}\right)^{1/\gamma} e^{i\pi/\gamma}, \quad \lambda_3^{(0)} = \left[\left(\frac{\pi^2}{4} + \frac{1}{D}\right) \frac{D}{\tau}\right]^{1/\gamma} e^{i\pi/\gamma}, \quad \lambda_4^{(0)} = \left[\left(\pi^2 + \frac{1}{D}\right) \frac{D}{\tau}\right]^{1/\gamma} e^{i\pi/\gamma}.$$

The last three points all lie on the same line, where

$$\cos(\gamma \arg \lambda^{(0)}) = -1 \quad \longrightarrow \quad \gamma \arg \lambda^{(0)} = \pi - 2\pi k, \quad k \in \mathbb{Z}.$$

Since none of the angles  $\frac{\pi}{\gamma} - \frac{2\pi k}{\gamma}$  belong to the principal branch, these three points do not contribute branch cuts. Only  $\lambda^{(0)} = 0$  is a relevant non-analytic point.  $\blacksquare$

Next, define  $\tilde{f}(\lambda^{(0)}) = f(\lambda^{(0)\gamma})$ , where  $f$  is defined in (48), so that  $\lambda^{(0)}$  is the root of  $\tilde{g} \equiv \tilde{C} - \tilde{f} = 0$ .

**Theorem A.1** Let  $\tau > 0$ . If the function  $\Re g \Big|_{\lambda^{(0)} = i\lambda_i}$  possesses a unique root  $\lambda_i^*$ , then for any  $D > 0$  the number of eigenvalues  $M$  of (48) in the open right half plane is either  $M = 0$  or  $M = 2$ .

PROOF Construct the contour as shown in figure 18 defined by

$$\Gamma_\varepsilon = \left\{ \lambda^{(0)} \mid \lambda^{(0)} = i\lambda_i + \varepsilon, \quad 0 < \varepsilon \ll 1, \quad -\infty < \lambda_i < \infty \right\} \cup \left\{ \lambda^{(0)} \mid |\lambda^{(0)}| = R, \quad R \gg 1 \right\}.$$

Note that the shift  $\varepsilon$  is unrelated to the activator diffusivity  $\varepsilon^{2\gamma}$ . By Proposition A.1 the function  $\tilde{C}(\lambda^{(0)})$  is analytic everywhere within  $\Gamma_\varepsilon$ . By Lemma 2.2 the operator  $\mathcal{L}_0$  has a positive eigenvalue  $\nu_{\text{loc}}$ , so that the function  $\tilde{f}(\lambda^{(0)})$  has a simple pole at  $\lambda^{(0)} = \nu_{\text{loc}}^{1/\gamma}$ . On the arc of  $\Gamma_\varepsilon$

$$\tilde{C}(\lambda^{(0)}) \sim \frac{\coth \theta_o}{\theta_o q m} \sqrt{\tau} \lambda^{(0)\gamma/2}, \quad \tilde{f}(\lambda^{(0)}) \longrightarrow 0, \quad \text{as} \quad |\lambda^{(0)}| \longrightarrow \infty.$$

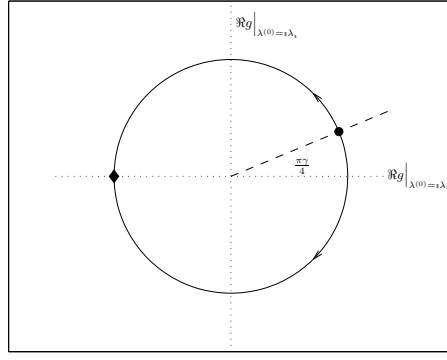


Figure 19: Argument winding paths in the calculation of number of eigenvalues in the right half plane.

Therefore

$$\arg g \Big|_{\substack{\lambda^{(0)}=\varepsilon\lambda_i \\ \lambda_i \rightarrow -\infty}} = -\frac{\pi\gamma}{4} \quad \arg g \Big|_{\substack{\lambda^{(0)}=\varepsilon\lambda_i \\ \lambda_i \rightarrow \infty}} = \frac{\pi\gamma}{4}. \quad (\text{A.1})$$

So the change in the argument along the arc is  $\frac{\pi\gamma}{2}$ . Using  $g(\lambda^*) = g^*(\lambda)$  ( the asterisk stands for complex conjugation ), the change of argument along the line  $\Re\lambda^{(0)} = \varepsilon$  is

$$\Delta \arg g \Big|_{\lambda_i \infty \searrow -\infty} = 2\Delta \arg g \Big|_{\lambda_i \infty \searrow 0}.$$

Altogether by the argument principle,

$$\Delta \arg g \Big|_{\Gamma_\varepsilon} = 2\Delta \arg g \Big|_{\lambda_i \infty \searrow 0} + \frac{\pi\gamma}{2} = 2\pi(M-1),$$

where  $M$  is the number of zeros in the right-half plane. Therefore,

$$M = \frac{1}{\pi} \Delta \arg g \Big|_{\lambda_i \infty \searrow 0} + \frac{\gamma}{4} + 1. \quad (\text{A.2})$$

By (A.1), the upper point of the line  $\Re\lambda^{(0)} = \varepsilon$  is in the first quadrant of the plane  $\left( \Re g \Big|_{\lambda^{(0)}=\varepsilon\lambda_i}, \Im g \Big|_{\lambda^{(0)}=\varepsilon\lambda_i} \right)$ , located on the line defined by the angle  $\frac{\pi\gamma}{4}$ . Since

$$\tilde{g}(0) = \tilde{C}(0) - \tilde{f}(0) = \frac{s+1}{qm} - \frac{1}{p-1} < 0$$

by the assumption on the GM model exponents, the mid-point is on the negative axis. Therefore the change in the argument is

$$\begin{aligned} \Delta \arg g \Big|_{\lambda_i \infty \searrow 0} &= \pi \left( 1 - \frac{\gamma}{4} \right) \quad \text{if } \Im g \Big|_{\lambda^{(0)}=\varepsilon\lambda_i^\dagger} > 0 \\ \Delta \arg g \Big|_{\lambda_i \infty \searrow 0} &= -\pi \left( 1 + \frac{\gamma}{4} \right) \quad \text{if } \Im g \Big|_{\lambda^{(0)}=\varepsilon\lambda_i^\dagger} < 0, \end{aligned}$$

where  $\Re g \Big|_{\lambda^{(0)}=\varepsilon\lambda_i^\dagger} = 0$ . Depending on the sign of the root  $\lambda_i^\dagger$  the imaginary axis is crossed either below or above the origin ( see figure 19 ). The proof is completed by using this result in (A.2) and then taking the limit  $\varepsilon \rightarrow 0$ . ■